ANALYSIS OF MICRO-STRAIN SENSORS BASED ON PHOTONIC CRYSTAL FIBERS

A Dissertation Submitted in partial fulfilment of the requirements for the award of the degree of

Masters of Engineering

In

Electronics and Communication Engineering

Submitted by

Shailly Khanna

Roll No. : 801361023

Under the guidance of

Dr. R. S. Kaler

Senior Professor and Deputy Director

Thapar University, Patiala

ELECTRONICS AND COMMUNICATION ENGINEERING DEPARTMENT

THAPAR UNIVERSITY

(Established under the section 3 of UGC Act, 1956)

PATIALA – 147004 (PUNJAB)

CERTIFICATE

I, Shailly Khanna, hereby declare that the work which is being presented in the dissertation entitled, **"ANALYSIS OF MICRO-STRAIN SENSORS BASED ON PHOTONIC CRYSTAL FIBERS"** by me in partial fulfillment of the requirement for the award of degree of M.E in Electronics and Communication submitted in Electronics and Communication Engineering Department of Thapar University, Patiala is an authentic record of my own work carried out under the supervision of **Dr. R. S. Kaler**, Senior Professor, ECED.

The matter presented in this dissertation has not been submitted in any other University/Institute for the award of degree.

Shailly Khanna

Date: 18-06-15

SHAILLY KHANNA

ROLL NO. 801361023

It is certified that the above statement made by the student is correct to the best of my knowledge and belief.

Date: 18-06-15

Dr. R. S. Kaler
Senior Professor & Deputy Director
Thapar University

Countersigned By:-

Dr. Sanjay Sharma
Professor & Head
ECED, Thapar University

Dr. S. S. Bhatia
Dean of Academic Affairs
Thapar University

ACKNOWLEDGEMENT

I would like to express my gratitude to **Dr. R.S. Kaler,** Senior Professor, electronics and communication engineering department, Thapar University, Patiala for his patience guidance and support throughout this report work. I am truly very fortunate to have the opportunity to work with him. He has provided help in technical writing, presentation style and I found this guidance to be extremely valuable.

I am highly grateful to **Dr. Sanjay Sharma**, Head, Department of Electronics and Communication, Thapar University, Patiala, for providing this opportunity to carry out the present work.

I also express my gratitude to **Dr. Amit Kumar Kohli,** P.G. Coordinator, Electronics and Communication Engineering Department, the entire faculty and staff members of Electronics and Communication Engineering department for their unyielding encouragement.

I am greatly indebted to all my friends, who have graciously applied themselves to the task of helping me with ample moral support and valuable suggestion. Finally, I would like to extend my gratitude to all those persons who directly or indirectly helped me in process and contributed toward this work.

Shailly Khanna

Roll No. 801361023

ABSTRACT

Photonic crystal fibers are a kind of fiber optics that present a diversity of new and improved features beyond what conventional optical fibers can offer. Due to their unique geometric structure, photonic crystal fibers present special properties and capabilities that lead to an outstanding potential for sensing applications. Photonic crystal fiber based sensors are characterized by high sensitivity, small size, robustness, flexibility and ability for remote sensing. Other advantages concern with the possibility to be used even in the presence of unfavorable environmental conditions such as noise, strong electromagnetic fields, high voltages, nuclear radiation, for explosive or corrosive media, and at high temperatures. These advantages in addition to their fabrication simplicity present them as a very efficient sensing solution for industrial, medical and environmental applications.

The objective of this dissertation is to analyze the performance of photonic crystal fiber based micro-strain sensors and for this purpose Opti-FDTD software is used which allows design of different configurations of photonic crystal fibers.

Firstly, a simple configuration of HC-PCF is presented for application as a micro-strain sensor to exhibit better sensitivity than the typical FBG-based fiber optic strain sensors. Also, cross-sensitivity to changes in surrounding refractive index is avoided. Secondly, a configuration of TC-PCF filled with a metal wire is proposed in order to improve coupling efficiency of fiber and application of such fiber for miniature micro-strain sensor configuration has been demonstrated. Thirdly, birefringence property of hybrid PCF structure is investigated and performance of Ge-doped HPCF as a micro-strain sensor is analyzed to achieve an enhanced value of sensitivity over other PCF based strain sensor configurations.

TABLE OF CONTENTS

CONTENTS **Page No.**

LIST OF ACRONYMS

DC-PCF	Dual Core Photonic Crystal Fiber
DFB	Distributed Feedback
EM	Electromagnetic
ESM	Endlessly Single Mode
FDTD	Finite Difference Time Domain
FBG	Fiber Bragg Grating
FLM	Fiber Loop Mirror
FLRD	Fiber-Loop Ring-Down
HC	Hollow Core
HC-PCF	Hollow Core Photonic Crystal Fiber
HPCF	Hybrid Photonic Crystal Fiber
MC-FPI	Micro-Cavity Fabry-Perot interferometer
mTIR	Modified Total Internal Reflection
MZI	Mach-Zehnder Interferometer
OF	Optical Fiber
OFS	Optical Fiber Sensor
OSA	Optical Spectrum Analyzer
PBG	Photonic Band-Gap
PC	Photonic Crystal
PCF	Photonic Crystal Fiber
PM-PCF	Polarization Maintaining Photonic Crystal Fiber
SC	Solid Core
SC-PCF	Solid Core Photonic Crystal Fiber
SHM	Structural Health Monitoring
SMF	Single Mode Fiber
SPR	Surface Plasmon Resonance
SRI	Surrounding Refractive Index
TC-PCF	Twin Core Photonic Crystal Fiber

UPML	Uniaxial Perfect Matching Layer

LIST OF FIGURES

LIST OF TABLES

CHAPTER-1

INTRODUCTION

There has been an incredible advancement and growth in the field of fiber optics over the last 25 years. In the beginning, these were considered as medium of carrying images and light for the purpose of medical endoscopy. Development of optical fibers after mid 1960s was mainly dedicated to the needs of the telecommunication industry. It is the result of extensive research in optical fiber technology, that huge amount of information and data can be transferred easily from one point to another in no time. Optical fibers have made a considerable impact in the areas of control, instrumentation and sensing also, through improvement of light guidance based high sensitivity controlled systems. Though, for application in these fields, fibers have to be made more sensitive and vulnerable to external conditions opposite to when utilized for telecommunication area, the fibers are required to be immune to the external mechanisms.

1.1 WHY SENSORS? WHY FIBER-OPTIC?

Sensing is a key technology for application areas like entertainment, transport, health and other industrial uses. Many such applications require the concept of remote sensors, where data is acquired from places which are not easily accessible. This concept requires three basic ingredients:

1. Sensor: A device which provides information about the physical/ chemical/ biological quantity of interest (e.g., pressure, temperature, pH etc.) by measuring it and translating into a format (e.g., electrical, optical etc.) that can be easily transmitted and processed.
2. Transmission lines
3. A platform to enable conversion of transmitted data into a format easily understood by human senses, i.e., displays that make the data visible or audible.

The transmission lines generally used are copper cables which leaves us with a choice of selection between the various types of available sensors. If we consider optical fibers as sensors, these allow interaction of parameters; physical, chemical, or biological; with light to generate a modulated optical signal containing information about the quantity to be measured. This format is easily accessed by the receiver with the help of a photodetector, which can convert light into the corresponding voltage or current. The basic reason that fiber-optic sensors are being given priority over the conventional sensors are [1]:

1. Transmission through electric cables suffers from the problem of external interference from electromagnetic fields. Optical fibers, in contrast, are immune to such kind of interference.
2. Optical fibers are small and light weight in comparison to electric cables. This comes as an advantage where miniaturization is crucial, e.g., in vehicles (spacecraft or aircraft industry).
3. Optical fibers are able to withstand extreme conditions of temperatures in comparison to electrical cables.
4. It is possible to multiplex fiber optic sensors effectively on a single network.
5. Optical fiber sensors open the gates for multifunctional sensing.

Thus, fiber optic sensors include all the advantages of optical fibers and thus are excellent contenders for environmental monitoring.

1.2 OPTICAL FIBER SENSORS

1.2.1 Operating Principle

A basic fiber optic sensing system includes a source of light, optical fiber, a transducer or sensing element and a detector. It depends on the type of sensor, whether intrinsic or extrinsic, that a separate transducer is used in the design or not. A fiber sensor operates by modulating one or more parameters of the system (e.g., wavelength, phase, intensity, polarization etc.) resulting in a change in the characteristics of the received optical signal at the detector [2]. Fig.1.1 shows a basic optical fiber sensing system, where the light from the source, guided through the optical fiber is subjected to interaction with an external quantity and the modulated optical signal is transmitted to the detector [3].

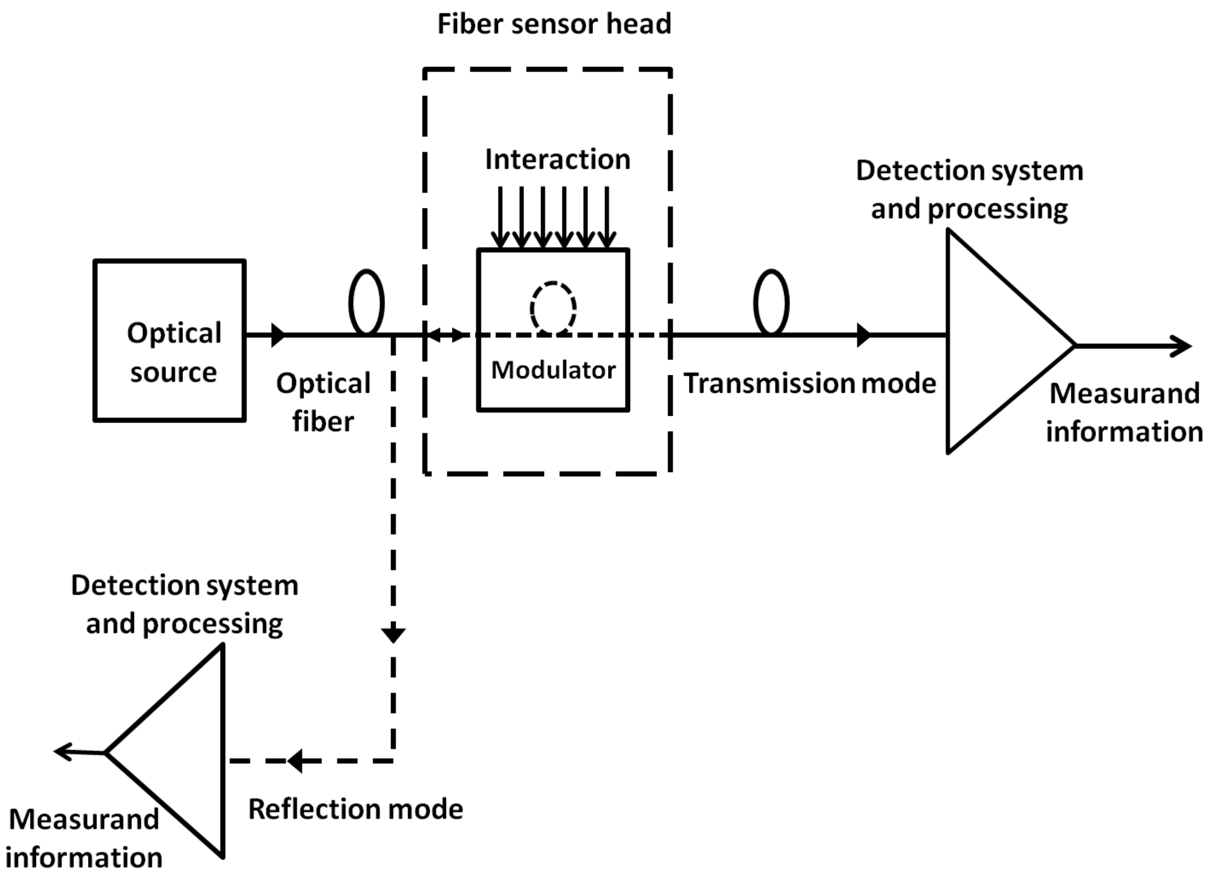

Fig.1.1 Basic block-diagram of fiber-optic sensor

The information about the input parameter can be gained from this modulated light signal. The sensor system can function in either reflection or transmission mode, depending on the type of sensor and its principle of operation. The sensing element or the optical fiber can have different variations. Variety of optical fibers have been used in the sensor design, long period gratings, fiber Bragg gratings, photonic crystal fibers, to name some. Each design has its own benefits over the other.

The optical sensors can not only sense through modulation of optical parameters but techniques have also been developed to sense the probing of matter by photons. The photons may either be scattered or absorbed. These techniques find great utilization in the field of chemical sensing.

1.2.2 Classification of Optical Fiber Sensors

Fiber optic sensor system can be classified in the following manner:

A. Based on sensor location [1]

   a) **Extrinsic sensors-** In these type of sensor systems, function of optical fiber is to carry light signal to a sensor, which can be placed in front of, next to, or near the fiber; to examine the measurand. Here, optical fibers act as the transmission medium and have no relation to acquired data.

   b) **Intrinsic sensors-** In these sensor systems, a part of fiber, or the fiber itself acts as the sensor for examination of measurand. There is no need of light leaving the fiber for acquisition of data, since fiber performs the function of sensor and cable simultaneously.

These sensors are shown diagrammatically in fig. 1.2 given below :

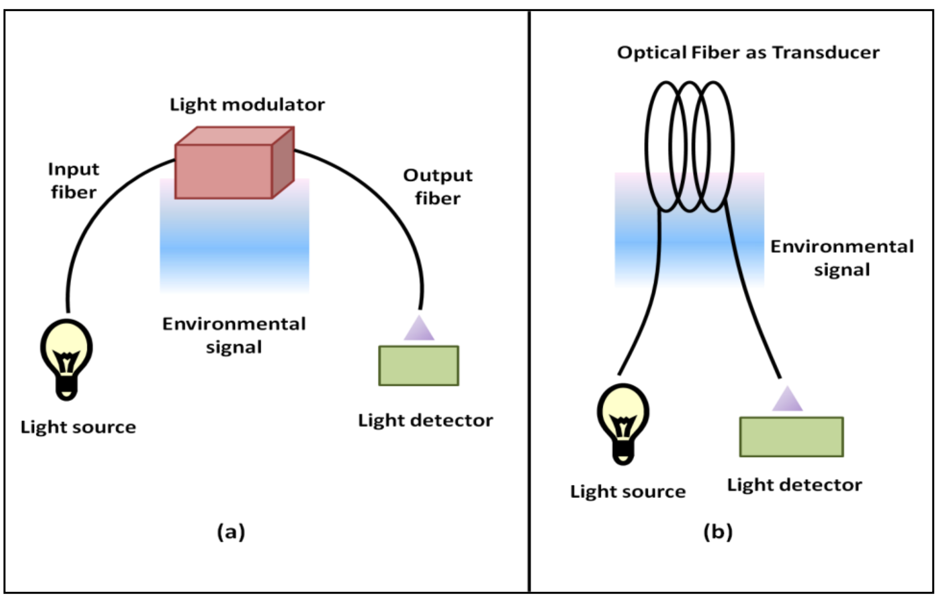

Fig.1.2 (a) Extrinsic sensor (b) Intrinsic sensor

B. Based on which characteristic of light is modulated by environmental changes

   a) Intensity
   b) Phase
   c) Frequency
   d) Polarization

C. According to the application
   a) Physical sensors- e.g., temperature, pressure, etc.
   b) Chemical sensors- e.g., pH content, spectroscopy, etc.
   c) Biological sensors- e.g., DNA, blood sampling, etc.

1.2.3 Fields of Application and Current Status

Fiber-optic sensors have grown rapidly in terms of quality and functionality and are being used widely in many areas like,

1. Pollution monitoring
2. Structural monitoring
3. Biomedical sciences
4. Biotechnology
5. Ground water monitoring
6. Process control
7. Titrimetry
8. Military/ aerospace
9. Electrical utilities/ power plants
10. Automation/ machines

Improved performance of optical fibers along with a decrement in price of optical fiber sensors has made these an attractive solution over conventional sensors. These fulfill demands which are application specific and are not satisfied efficiently with conventional sensors, e.g., high temperature and pressure monitoring in the oil and gas industry, which makes it a major market for fiber sensors. Aeronautical and civil engineering sectors are also getting benefitted as fiber-optic sensors can ensure safety improvement by giving beforehand warning of critical failures in buildings and structures. Embedding fiber optic sensors with smart structures boosts the safety of advanced structures, machines and devices [3].

1.2.4 Issues with Optical Fiber Sensors

Though optical fibers present many benefits over the conventional sensors, some concerns accompany this technology as well. These include issues like [2],

1. Cost: Optical fiber sensors are costlier than conventional electrical-based sensors.
2. Ambient light: In an optical fiber sensor, ambient light can interfere with the signal of interest. Thus, measurements should be carried out in dark.
3. Response time: Response time of sensor can be long, particularly in case of multiphase sensing techniques.
4. Long-term stability: Since optical fiber technology is still in its initial state, very less amount of information is available about its performance in the long run and reliability.
5. Dynamic range: Operating dynamic range of fiber optic sensors may be smaller than that of electronic sensors.
6. Data interpretation: The analysis of data acquired from the sensors may not be straightforward since output is subjective to changes due to other parameters. Thus the effect of other parameters on the output should be controlled.

1.3 FROM CONVENTIONAL OPTICAL FIBERS TO PCF

PCFs constitute an emerging class of optical fibers and combine properties of photonic crystals and optical fibers into one, so as to exhibit properties not possessed by conventional optical fibers. PCF geometry is characterized by a periodic arrangement of air-filled capillaries running along the entire length of the fiber, centered on a hollow or solid core [4]. The difference between conventional OF and PCF lies in the fact that waveguide properties of PCF are not due to varying composition of glass, as in later, but due to its internal periodic structure of air holes.

Even though conventional OFs present an excellent performance in fiber telecommunication and have many advantages over standard sensors, there are some restrictions which have limited the use of optical fiber as sensors. Some of them are stated below [5]:

1. The selection of material for fabrication of the core and the cladding is restricted as thermal, optical and chemical properties of both the materials should match with each other.
2. The refractive index profile and the geometry of OFs limit characteristics such as, dispersion, inherent losses, birefringence and non-linearity to be freely engineered so as to make advancement in field of fiber sensors.

So, there was a need to explore additional options in the field of fiber optic technology to involve the advantages of optical fibers in various fields by overcoming their limitations. The invention of PCFs became a breakthrough in optical fiber technology due to possession of extraordinary properties, enabling them to overcome many limitations faced by conventional OFs.

1.4 GEOMETRY, LIGHT GUIDANCE MECHANISMS AND CHARACTERISTICS OF PCFS

Standard SMFs consist of a doped core which is surrounded by a pure silica cladding as shown in fig.1.3(a). Refractive index of the core must be higher than that of the cladding for proper guidance of light. As discussed earlier, PCF geometry entails cladding composed with air capillaries, centered on a hollow or solid core. Thus, PCFs are divided into two categories on the basis of their geometry [4]:

1. **Solid-core PCFs**- The cross-section of SC-PCFs include periodically arranged air capillaries around a solid core. This kind of geometry helps in lowering the effective refractive index of the cladding, when a single material is used for manufacturing. A general SC-PCF is shown in fig. 1.3(b).
2. **Hollow-core PCFs**- As suggested by the name itself, HC-PCFs consist of a central hollow (air) core with cladding also made up of air-holes. These present a negative core-cladding refractive index difference. Fig.1.3(c) shows an illustration of HC-PCF.

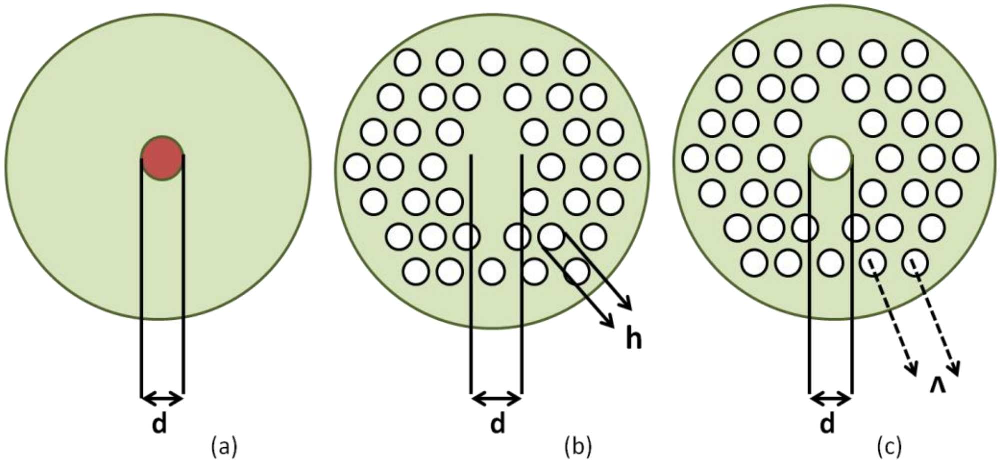

Fig.1.3 Cross sectional geometry of (a) SMF (b) SC-PCF (c) HC-PCF

For an SMF, core diameter is the only parameter to be taken into account, whereas, in case of a PCF, three physical factors must be taken into consideration: the diameter of the core, d (for SC-PCF, diameter of ring constituted by innermost layer of air-holes), diameter of air-holes of cladding, h and the pitch, Λ, which is the distance between centers of two adjacent air holes [4]. Thus, by varying these constraints in combination with the preference of material refractive index and the lattice geometry, properties of PCFs can be managed. Hence, designing and fabrication of PCFs becomes very flexible. Such liberty of structural modification is not possible with conventional OFs.

There are different mechanisms by which light can be guided through a PCF: modified TIR and/or PBG. There are four different guidance mechanisms depending on the geometry of PCF and selection of core/cladding material [6]:

a) **PBG-guiding PCF**: light is confined in the core through PBG effect in the hollow core
b) **Index-guiding PCF**: light is confined in the solid core through mTIR
c) **Hybrid PCF**: guides light through simultaneous PBG and mTIR phenomenon
d) **All-solid PBG PCF**: guidance in a solid core through PBG antiresonant effect

1.4.1 Index-Guiding PCFs

The cross section of these PCF illustrate an array of air holes periodically arranged around a central solid core. As the cladding and the SC are made up of a single material, there occurs a reduction in the effective refractive index of the cladding, thus exhibiting the phenomenon of mTIR for light guidance through core. Here, doping of the core is not required, instead special arrangement of air holes does the same job. For a conventional OF, the V-number is affected by two parameters: operating wavelength, λ and the core radius. But in case of index-guiding PCF, an extra parameter adds up in the equation, i.e., V-number also depends on how the air holes are arranged in the cladding [7], [8].

$$V_{IG-PCF} = \frac{2\pi}{\lambda}\Lambda\sqrt{n_{co}^2 - n_{eff(cl)}^2} \qquad (1.1)$$

As already known, V-number keeps on increasing without any limit, if λ is decreased or size of the core is increased. PCFs present a different behavior for this. For shorter range of wavelengths (λ~d), V_{IG-PCF} has a finite value and does not depend on either λ or Λ, while at longer values of λ, the optical field present in the cladding region may be modulated weakly by the air holes [9]. Due to this unique behavior of PCFs, mono-mode guiding is likely to achieve over a major portion of the transmission window. This gives rise to a special feature of SC-PCFs, endlessly single mode guidance. ESM is characterized by the fill factor (d/ Λ ratio) in order to maintain $V < V_{IG-PCF}$ [7], [9].

1.4.2 PBG-Guiding PCFs

The cross section of these PCF illustrate an array of air holes periodically arranged around a central hollow core resulting in a negative core-cladding refractive index difference, which makes it impossible to guide light through TIR. However, a proper design of the photonic crystal cladding can enable the confinement of light in the HC. The periodic arrangement of air holes gives rise to a 2-D photonic crystal geometry having lattice constant similar to λ. PBGs exist in such crystals, that do not allow light of particular frequency range to propagate through the crystal. A unique region can be created, with different optical properties; if a defect is introduced to break the periodicity of the structure. This region allows modes with frequencies lying inside the PBG, to propagate, but the light is confined near the defect region only. The modes which lie outside the defect region undergo refraction and rest of the modes are guided through the hollow core of the fiber. See for example, fig. 1.4, where a HC-PCF designed for red light is illustrated and does not guide light of any other color [2], [5].

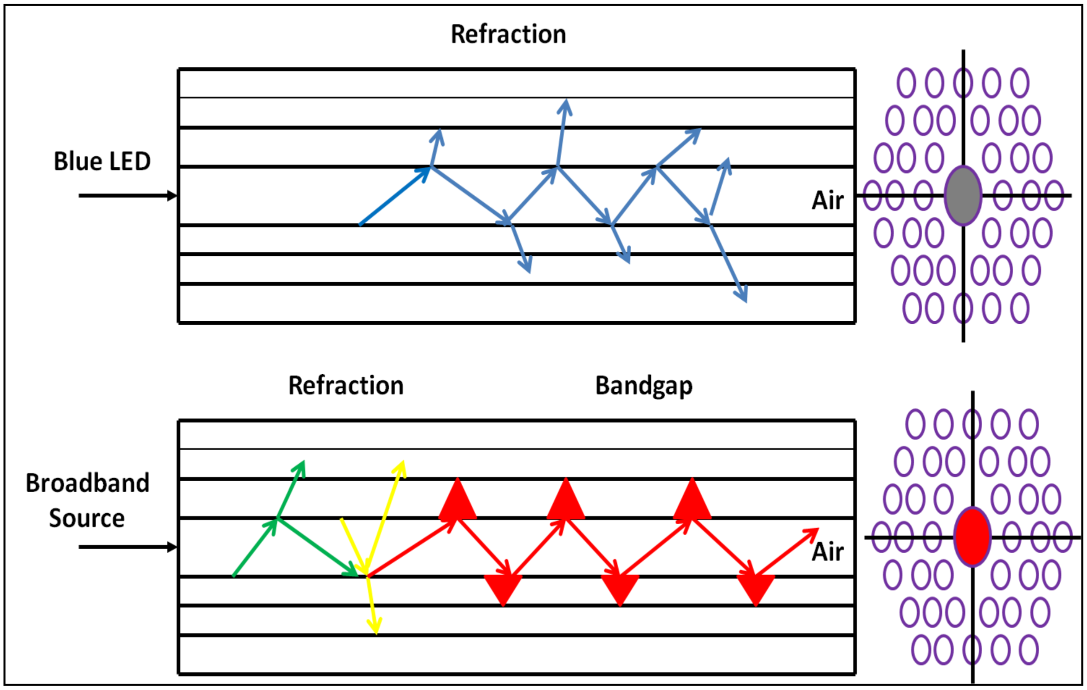

Fig. 1.4 PBG-guiding through HC-PCF

1.4.3 All Solid PBG-PCFs

Even though, PBG support guidance of light through air, this effect may also be experienced in a SC. Light guidance through PBG effect can be observed in a SC-PCF through proper arrangement of solid inclusions, having a higher refractive index than the core. The first all solid PBG-PCF was reported in 2004 [10], where bandgap was formed as a result of anti-resonances of high-index strands present in the cladding. Fig. 1.5 shows an illustration of a all solid PBG-PCF.

The PBGs of the cladding material establish the transmission properties of solid PBG-PCFs, described by the ARROW model [11]. The spectral transmission through core appear as a number of low- and high-loss regions due to exclusion of higher-order cladding modes [12].

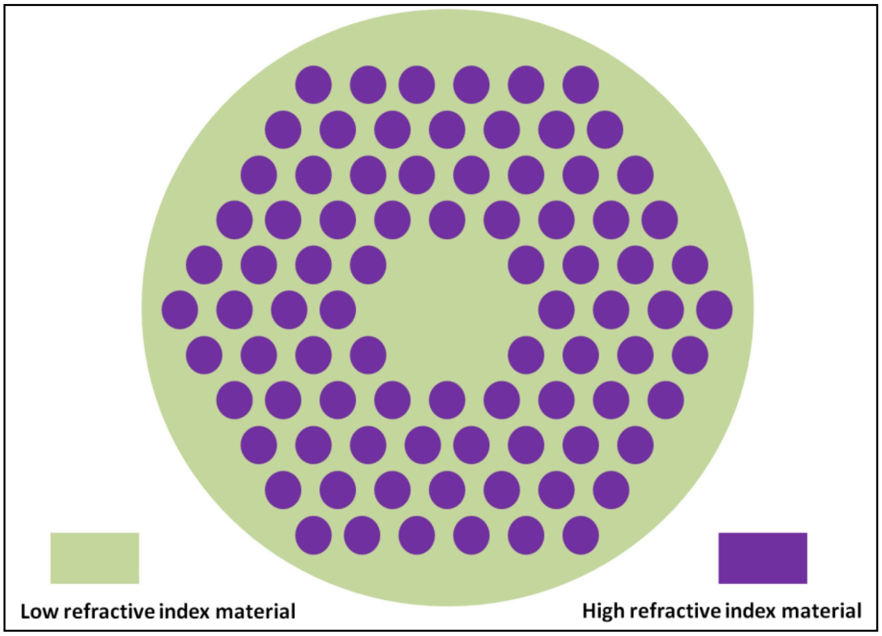

Fig.1.5 Diagrammatical representation of all solid PBG-PCF

1.4.4 Hybrid PCF

A hybrid PCF exhibits both the guidance mechanisms: PBG and mTIR simultaneously. Although, light guidance through hybrid mechanism was already reported in other waveguides [13], the first hybrid PCF structure was reported in 2006 [14]. The structure consisted of hexagonal arrangement of air holes and a row of holes in the centre was composed of a material with higher refractive index than silica core as shown in fig.1.6

With reference to fig.1.6 the phenomenon of light guidance through a hybrid PCF can be explained as [14]:

- Along y-axis: the core-cladding refractive index is positive, hence, the light is guided through mTIR
- Along x-axis: negative core-cladding refractive index difference exists, making TIR unfeasible. Thus, light is guided in limited frequency bands overlapping with PBGs, which appear at antiresonant states of the of the solid inclusions.

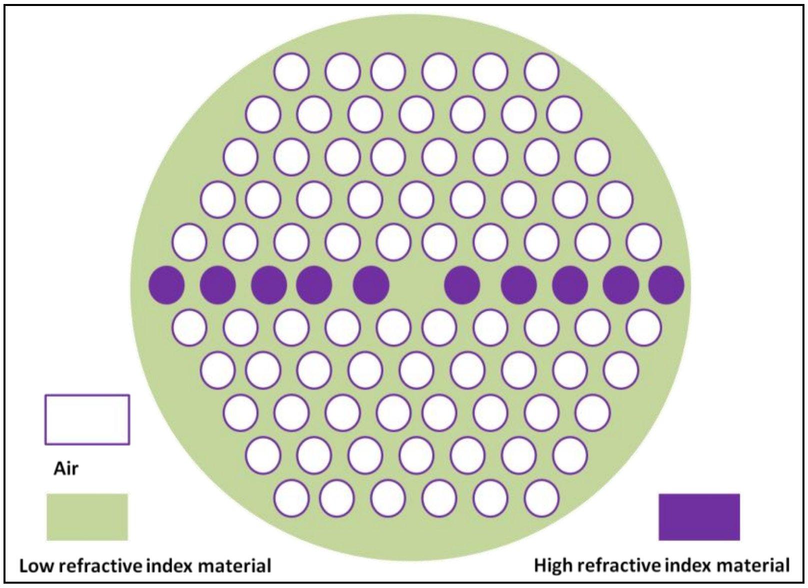

Fig. 1.6 Diagrammatical representation of hybrid PCF

The hybrid PCFs provide a great flexibility of design in terms of adjusted birefringence, which finds great application in the sensing field.

1.5 MODELING OF PHOTONIC CRYSTAL FIBER

The methods used to model conventional OFs cannot be used in modeling of PCFs due to their large refractive index disparity and a subwavelength periodical geometry. Thus, techniques to model PCs and EM fields are adapted to this purpose.

The FDTD method is extensively applied for calculating the evaluation of an EM field in depressive media [15]. The wave propagation through the PCF structure is found by direct integration in the time domain of Maxwell's equations in a discrete form. Space and time is discrete in a regular grid. Evaluation of the electrical and magnetic field is calculated on a Yee cell (fig.1.7). In addition, the boundary conditions are added (absorbing or periodic ones). Most often UPML boundary conditions are used for PCF modeling. The method allows obtaining transmission and reflection coefficients, energy flow of propagation fields (Poynting vector). It allows the observation of a steady state field distribution as well as the temporary field distribution.

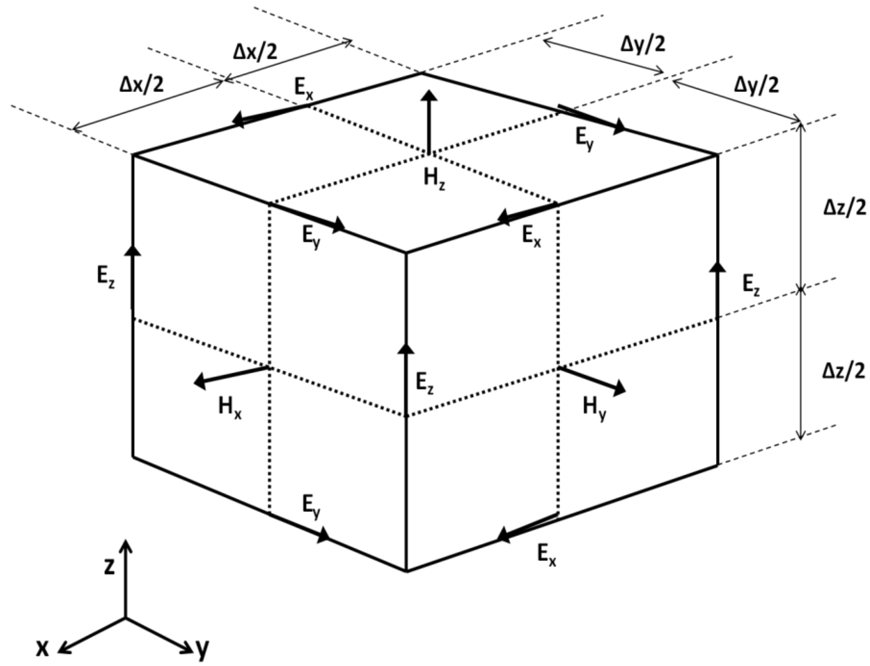

Fig.1.7 Yee cell

The FDTD method is universal, robust, and methodologically simple. Though, a negative aspect of this algorithm is its large value of time and memory complexity. Also, simulation is possible for only short length of PCF with this method, as, PCFs have 3D geometry with refractive index variation in 2D. Although, simulation of large volumes can be done with computer clusters because the FDTD method can easily be executed as a parallel algorithm.

1.6 APPLICATIONS OF PCF IN SENSING

PCFs find application in sensing because it provides more parameters which can be varied, as compared to the standard optical fibers. Some of these parameters are

1. The number, size and shape of the cladding holes and/or the core
2. Mode shape
3. Fiber transmission spectrum
4. Dispersion
5. Non linearity
6. Fill factor

7. Birefringence

Any of these parameters can be tuned to achieve values which are not attainable with standard optical fibers. Also, the presence of air holes in the cladding allows light propagation in air or insertion of gases/liquids into them. This provides a well controlled interaction environment between the sample and the light inside the fiber only, which was not possible with conventional OFs [16].

The application of PCFs in the sensing field allocates new possibilities and improved solutions in the field of physical, chemical and bio-sensing. PCFs have demonstrated their ability to succeed in harsh environments which are present in sensing of some physical quantities like pressure and temperature. Also, in bio-sensing, PCFs can work with a very small amount of the sample as compared to conventional OFs, which paves the way for new technology in the field of DNA recognition etc.

1.7 SENSORS FOR STRAIN MONITORING OF COMPLEX STRUCTURES

Strain monitoring is necessary for civil structures to detect any kind of damage or variation in their structural characteristics so that they can be easily rectified at an early stage. SHM is a widely researched field these days. The main focus is on development of such sensor arrays which can be integrated to function similar to human nervous system and are able to sense even minute levels of strain by avoiding cross sensitivity to external parameters [17]. Relatively light- weight structures, with ability to tolerate large amount of load, can be produced with the help of composite structures as these possess the benefits like: high structural performance, large strength/weight ratio and corrosion resistance. Though, these materials also have negative aspects, like, these are prone to matrix cracking and delamination, which may cause a decrease in strength of the overall structure [18]. These processes are initiated by appearance of excessive residual strains in composite materials to cause noticeable distortion and untimely failure of the structure. The phenomenon which are mainly responsible for generation of residual strains are [19]:

1. Chemical contraction of matrix

2. Disparity between the thermal expansion coefficients of the constituent materials

Thus, there is a need of in-situ measurement techniques to avoid or minimize the generation of residual strains in composite materials which in turn, demands for development of sensors which can directly monitor the generation of internal strain throughout the cure process of composite materials.

Many sensing techniques, including fiber optic sensor based systems, have been proposed for strain monitoring of complex structures. These mainly include development of FBG-based sensors, which have advantage of small dimension to be easily embedded inside composite materials avoiding any distortion to the structure. But, they also possess cross-sensitivity to temperature to a great extent and exhibit a contrast in thermal expansion coefficients of core and cladding materials [19]. PCFs have emerged as an attractive solution to these problems, as they are made up of a single material, thus solving the problem of mismatching of thermo-optic coefficients of the materials. Also, cross-sensitivity to temperature is resolved up to a limit as air holes have a zero thermo-optic coefficient. Additionally, PCF based sensors are compact in nature and are easy to fabricate.

1.8 OBJECTIVES OF DISSERTATION

1. To design and simulate operation of PCF as a micro-strain sensor and control its cross sensitivity to external parameters.
2. To design a structure of PCF to be used as a miniature strain sensor with lower coupling losses
3. To improve strain sensitivity by utilizing birefringent properties of PCF

1.9 ORGANIZATION OF DISSERTATION

Chapter 2 gives literature survey about the topic of the dissertation. In order to start the dissertation, the first step is to study the research papers that have already been published. Research papers related to this work are chosen and studied. Literature review helps in analysis of work already done and defining the scope to make work easier.

Chapter 3 presents an investigation of HC-PCF to be used as a micro-strain sensor which is insensitive to variations in refractive index of surroundings.

Chapter 4 presents the application of TC-PCF filled with Ag wire as a micro-strain sensor with a improved sensitivity and a high coupling efficiency.

Chapter 5 analyses the use of birefringent properties of PCF to enhance sensitivity to strain with help of hybrid PCF structure which guides light by both mTIR and PBG guiding mechanisms.

Chapter 6 includes the conclusion, recommendations and future scope of the work.

CHAPTER-2

LITERATURE SURVEY

Recently, much interest has been shown in the use of optical fibers for sensor applications due to their offered advantages over conventional electrical sensors. PCF based sensors have gained much interest lately, as depicted in this chapter. There has been a growing need of cost effective and highly sensitive micro-strain sensors for various strain monitoring applications.

As exhibited in this chapter, many researchers have worked on development of highly sensitive PCF-based micro-strain sensors. Some authors have used interferometer technique by applying different methods for collapsing of air holes in order to enhance strain sensitivity while others tried to improve the sensitivity through use of FLMs. A great research has been done for reducing the cross sensitivity of the strain sensors to external parameters.

The literature survey of PCF-based micro-strain sensors by various researchers in past years is shown below:

J. Villatoro *et al.* [20] in **2006** demonstrated a strain sensor which was based on a large-mode-area PCF. Tapering of the fiber was done in order to allow collapsing of air holes. This process made the fiber more sensitive to environmental parameters. Also, it caused transformation of the taper waist into a solid multimode fiber initiating the coupling between the various generated modes of the fiber. Consequently, a sequence of interference peaks was observed in the transmission spectrum of the sensor device. Application of longitudinal strain to the taper caused these interference peaks to shift towards shorter wavelengths, linearly. The device exhibited temperature insensitivity, since no shift in the spectrum was observed when temperature conditions varied from 0°C to 180°C. The reported sensor was able to operate at numerous wavelengths and was reversible in nature.

J. Villatoro *et al.* [21] in **2007** reported strain sensing facilitated by a PCF spliced to two standard OFs. The air holes of the PCF were collapsed over a short section to convert it into a solid all-silica fiber, which resulted in broadening of propagating modes of the lead-in fiber, subsequently allowing intermodal coupling only between two modes in the fiber. The reported sensor sensitivities of 2.80 pm/ με at 1550 nm and 1.45 pm/ με at 850 nm were comparatively higher than that obtained by Bragg grating-based strain sensors. A small error of ~1.5 με/°C in strain measurement was encountered due to temperature fluctuations. Thus, for normal environment operation, the sensor demanded no need of temperature compensation. The device showed attractive features like wavelength-encoded information, entirely linear response, wide range of operating wavelengths, high thermal insensitivity, and easy fabrication. The proposed device was useful in different applications where physical parameters like vibration, load etc. could be transformed to strain changes.

O. Frazao *et al.* [22] in **2007** worked on development of Hi-Bi PCF-based strain sensors with high temperature insensitivity. Wavelength-based measurement was exploited to sense the changes in strain. The Hi-Bi PCF loop mirror was analyzed for two different cases: uncoated and acrylate-coated PCF. It was observed that coating the PCF helps in minor increase in the strain sensitivity (1.21 pm/ με) as compared to that achieved with the uncoated one (1.11 pm/ με). The device was reported as insensitive to temperature changes with a low sensitivity of 0.29 pm/K.

Q. Shi *et al.* [23] in **2008** designed a strain sensor which was insensitive to temperature and bend. This kind of strain sensing was accomplished with help of miniature in-line Fabry-Perot interferometers through splicing of a small piece of HC-PCF between two SMFs. As the HC-PCF guides the light through air, the temperature-induced variations in strain were small, owing to almost zero thermo-optic coefficient of air. Also, small length of PCF was used which made bending of fiber difficult, to observe negligible spectrum shift of the reflected signal due to bending. The proposed design was able to achieve high strain sensitivity of 1.55 pm/ με and was highly stable to external changes.

Y.G. Han [24] in **2009** proposed strain measurement based on a PM-PCF. He was able to achieve periodic transmission (wavelength dependant) in a birefringent interferometer by placing a piece of PM-PCF in between two linear polarizer. Since, very less change in the birefringence of PM-PCF was observed when temperature was varied, negligible shift was detected in the peak wavelength of the spectrum. This resulted in a low sensitivity of – 0.3 pm/°C with temperature. Though, a proportional shift in peak wavelength was observed on application of longitudinal strain on the device. A strain range of 0 to 1600 με resulted in a high strain sensitivity of 1.3 pm/ με with an estimated resolution of 2.1 με. This simple structure included benefits like easy installation, and low loss without a Sagnac loop and a shorter sensing probe.

W. Qian *et al.* [25] in **2010** developed a low-cost temperature-insensitive strain sensor based on Hi-Bi PCF loop mirror. Intensity-based measurement was exploited to achieve a low temperature sensitivity of 0.0027 dB/ με since the position of resonant dip was least affected by the variations in temperature. However, linear shifting of the resonant dip towards longer wavelengths was observed with the stretching of the fiber, as phase matching condition changes due to applied strain. A DFB laser was used as the source of light. An optical power meter was found sufficient to measure changes in output intensity of FLM with application of strain, thus eliminating the need of an OSA, making the design cost effective.

W. Zhou *et al.* [26] in **2011** demonstrated a highly sensitive strain sensor obtained through combination of PCF-MZI with FLRD technique. A short length of PCF was spliced between two SMFs in order to fabricate the MZI. The air holes near the two splicing points were collapsed in order to facilitate coupling between the core and cladding modes inside the PCF. The decay constants of the FLRD cavity were measured for different values of axial strain to obtain a high strain sensitivity of ~2.1 μs^{-1}/mε with a strain resolution of ~3.6 με. The proposed strain sensor system offered high detection speed and lower cost, thus finding application in instrumentation field.

L.M. Hu *et al.* [27] in **2012** proposed and experimentally demonstrated a temperature in-sensitive strain sensor based on a modified PCF-MZI, by introducing a collapsed region in the middle of the PCF for improvement of extinction ratio. The modified MZI consisted of total three collapsed regions as the index-guiding PCF section of short length was longitudinally sandwiched between two SMFs. Intensity-based measurement was employed to achieve a strain sensitivity of 11.22 dB/mε over a range of 1.28 mε and a strain resolution of 0.89 με. The sensor system exhibited high temperature stability and proved cost efficient.

W. Peng *et al.* [28] in **2013** proposed and experimentally demonstrated a high-sensitivity hybrid fiber-optic strain sensor based on a structure combining a MC-FPI and a MZI. The two ends of the PCF were spliced to conventional SMFs. Splicing parameters were controlled such that lead-in SMF/PCF functioned as a mode splitter/combiner by forming a micro-cavity through collapse of air holes. However, no micro-cavity was formed for lead-out SMF/PCF and splicing point acted as mode splitter and combiner. The sensor was able to operate in both transmission and reflection modes. The strain was detected by measurement of wavelength separation of the two resonance dips with one in the reflection spectrum and the other in the transmission spectrum. The change in wavelength separation was linearly proportional to the applied strain, which generated a maximum strain sensitivity of 8.69 pm/με. Moreover, the sensor possessed good photosensitivity but demonstrated polarization independency.

S.R. Rodrigo *et al.* [29] in **2013** presented a configuration of strain sensor based on Hi-Bi PCF, which acted as a sensing head to enable measurement of interferometric signals in-reflection. The operating principle of the investigated sensor depended on two properties of Hi-Bi PCF: high thermal stability and high birefringence. Light propagation through sensor generated a shift between the two birefringent axis which was sensed by the sensing head of the device. Thus, by monitoring the shift in interference wavelength, strain measurement was accomplished. The proposed system was cost effective as sensing head interrogation was made through the laser, thereby experiencing power shifts due to strain variations to attain a high strain sensitivity of 7.96 dB/mε. The sensor head was able to bear high values of strains; rupture point was observed near to 5000 με. Due to in-reflection measurements, the proposed system was found helpful for strain measurements in hazardous environments.

J. Zheng *et al.* [30] in **2013** worked on fabrication of a simple, compact and low cost MZI strain sensor with the help of a PCF fusion spliced to two conventional OFs. The method of collapsing of air holes was applied to an index-guiding PCF to induce interference between the core-guiding mode and higher order core mode, instead of cladding mode. The sensor showed linear response to variations in strain levels and achieved a sensitivity of 2.1 pm/ $\mu\varepsilon$ for MZI length of 45 mm at wavelength 1550 nm. It was observed that the length of the PCF has a negligible effect on the strain sensitivity. The proposed sensor structure was able to overcome the effect of cross sensitivities to SRI and temperature variations. A relatively low temperature sensitivity of 13.24 pm/°C was reported with the sensor making it attractive solution for various sensor applications.

F. Xu *et al.* [31] in **2014** proposed and experimentally demonstrated MZI type strain sensor designed through splicing of a DC-PCF to two SMFs. The MZI pattern was observed in the sensor due to the difference in modal indices of the two fiber cores. The authors were able to quantitatively control the length of the DC-PCF but the discharge arc conditions required for fusion splicing were not under control. The mode coupling between the two fiber cores was ignored due to relatively large spacing between the two cores due to the air hole. Longitudinal strain was applied to different lengths of DC-PCF and transmission spectrum was monitored to observe a red-shifting for increasing levels of strain in all cases. The measured sensitivities were 1.9 pm/ $\mu\varepsilon$ for length 4 cm and 1.4 pm/ $\mu\varepsilon$ for 2 cm length indicating that a longer DC-PCF tends to have a higher strain sensitivity. Since, the DC-PCF comprises of only temperature-resistant fused silica, the proposed sensor was beneficial in the field of ultra-high temperature sensing.

X. Bai *et al.* [32] in **2014** experimentally demonstrated a PCF in-line MZI structure (PMS) for a fiber ring cavity laser based strain sensor. The PMS was employed as an optical band-pass filter to function as a strain sensing element. The role of fiber ring cavity was to improve the resonant spectrum visibility, and narrowing the corresponding 3-dB bandwidth, thus resulting in an overall enhancement of sensing performance. The lasing wavelength as well as the transmission spectrum observed a blue-shift on application of increasing levels of axial strain. A high strain sensitivity of 2.1 pm/ με was achieved in the linear range of strain 0-2100 με, while neglecting the temperature sensitivity when operating in normal environment. The sensor presented approximately 9 times increase in the value of quality factor as compared to previously reported PCF-MZI sensors, thereby proving useful in long-distance axial strain sensing.

Table 2.1 Literature survey

S. No.	AUTHORS	YEAR	WORK DONE	RESULTS
1.	J. Villatoro *et al.*	2006	Use of large-mode-area PCF and tapering process for collapsing air-holes	Temperature insensitivity
2.	J. Villatoro *et al.*	2007	Use of SMF-PCF-SMF structure through collapse of air holes over a short section of PCF to allow intermodal coupling between two modes only	Higher strain sensitivity than Bragg-grating based sensors
3.	O. Frazao *et al.*	2007	Use of Hi-Bi PCF loop mirror for strain sensor and analysis of uncoated and acrylate-coated PCF	Coating the PCF increases strain sensitivity
4.	Q. Shi *et al.*	2008	Use of HC-PCF for in-line Fabry-Perot interferometer based strain sensor	High strain sensitivity and insensitivity to temperature and bend

5.	Y.G. Han	2009	Use of PM-PCF to observe change in birefringence with strain and temperature	Increase in strain sensitivity and resolution and reported low losses without Sagnac loop
6.	W. Qian *et al.*	2010	Use of intensity based-interrogation for strain sensor based on Hi-Bi PCF loop mirror	Low temperature sensitivity and eliminated need of OSA to make design cost effective
7.	W. Zhou *et al.*	2011	Combined PCF-MZI with FLRD technique to obtain high strain sensitivity and resolution	High detection speed for utilization in instrumentation field
8.	L.M. Hu *et al.*	2012	Experimentally demonstrated temperature insensitive strain sensor based on modified PCF-MZI	High temperature stability and higher sensitivity to strain
9.	W. Peng *et al.*	2013	Proposed a hybrid sensor structure combining MC-FPI with MZI to be operated in both transmission and reflection modes	Improved strain sensitivity and polarization independency
10.	S.R. Rodrigo *et al.*	2013	Presented in-reflection measurement of interferometric signals with help of strain sensor based on Hi-Bi PCF	High strain sensitivity with ability to bear large values of strain

11.	J. Zheng *et al.*	2013	Fabricated a low cost MZI strain sensor with help of SMF-PCF-SMF structure	High sensitivity to strain and insensitive to SRI and temperature variations
12.	F. Xu *et al.*	2014	Use of DC-PCF made with temperature-resistant fused silica for MZI type strain sensor	Higher strain sensitivity was observed with a longer DC-PCF
13.	X. Bai *et al.*	2014	Use of PMS structure for a fiber ring cavity laser based strain sensor to improve resonant spectrum visibility	Around 9 times improvement in value of quality factor

CHAPTER-3

INDEX INSENSITIVE MICRO-STRAIN SENSOR BASED ON HOLLOW CORE PHOTONIC CRYSTAL FIBER

HC-PCF undergoes PBG guidance when light is launched into the fiber. Since, PBG is sensitive to external parameters, HC-PCF can be designed to function as a micro-strain sensor. The main benefits of HC-PCF based strain sensor include simple geometry, easy fabrication and compact structure for in-situ measurements. The performance of the designed sensor is investigated for different strain levels ranging from 0 με to 2000 με at the wavelength, 1550 nm. Additionally, due to the special air-hole structure of HC-PCF, the sensitivity of strain measurement remains unaffected of the changes in SRI. Sensitivity of HC-PCF also depends on the fiber parameters like pitch, air-filling fraction etc. as shown in this chapter.

3.1 INTRODUCTION

Optical fiber sensors have emerged as a unique solution in particular cases (e.g., in environments with electrical hazard or potentially explosive). Although, sensors based on conventional optical fibers are well established [33], PCF, despite of its youth in sensing field has gained attention of the researchers. PCF is a recently developed class of optical fiber [34] which are characterized by periodic arrangement of air-filled capillaries running along entire length of the fiber, centered on a solid or a hollow core. The biggest attraction in PCFs is that by varying the size and location of the holes of the cladding and/or the core, the transmission spectrum, mode shape, dispersion, birefringence etc. can be tuned to reach values which are not possible with conventional optical fibers. PCFs turn out to be a promising and enhanced solution for practical applications where monitoring of strain-induced changes is important, such as, in the fields of experimental mechanics, metallurgy, aeronautics, and significantly, in health monitoring of complex structures [4].

Q. Shi *et al.* [23] obtained a strain sensitivity of 1.55 pm/με and insensitivity to temperature and bend, with the help of Fabry-Perot-type strain sensor based on HC-PCF. B. Dong *et al.* [35] proposed a modal interferometer based micro-displacement sensor constructed with help of SMF-PCF-SMF structure to achieve a strain sensitivity of ~0.0024 dB/μm and a low temperature sensitivity. H. Gong *et al.* [36] presented a modal interferometer based on short length PCF for strain measurement to achieve a strain sensitivity of 1.83 pm/με.

In spite of the vast research in the field of strain sensing using PCF, it has not lead to commercialization of PCF sensors. So, techniques have to be developed so as to make PCF sensing more cost effective. Also, strain sensitivity needs to be increased in order to measure comparatively lower magnitudes of applied strain. This can be done by manipulating the geometry of the PCF, e.g., by varying the core diameter or by changing the pitch of the fiber in order to obtain a higher sensitivity. Insensitivity to temperature is an issue which has mostly been researched upon in the past. PCF sensors which can also avoid the cross sensitivity to other parameters, e.g., changes in SRI, vibration, bend etc, have to be designed.

In this chapter, we have presented two different structures of HC-PCF which differ in their core diameters (large core and small core) and demonstrated their application as a strain sensor. The FDTD method is used to simulate operation of sensor at different strain levels. Comparison of the strain sensitivities of the two fibers has been done. Insensitivity of this sensor to the changes in SRI has also been verified.

This chapter has been divided into four sections. The section 3.2 explains the basic principle of strain sensing based on HC-PCF. It also describes the simulation set-up of HC-PCF based strain sensor. The section 3.3 gives the discussion of the results observed after the simulations. The section 3.4 gives the conclusion about utilizing HC-PCF for the purpose of strain sensing.

3.2 THEORY AND SIMULATION SETUP

A PCF is made up of two materials which have a high contrast of refractive index. Thus, it can be referred to as a 3D structure having a 2D refractive index distribution such that the light remains confined to the core. When light enters a HC-PCF, the fundamental core mode is spread widely, and higher order modes, including the cladding modes, are excited in the PCF. The total intensity can be calculated as [21]:

$$I(\lambda) = I_{co}(\lambda) + I_{cl}(\lambda) + 2[I_{co}(\lambda)I_{cl}(\lambda)]^{1/2}\cos\left(\frac{2\pi\Delta nL}{\lambda}\right) \tag{3.1}$$

where, I_{co} (λ) and I_{cl} (λ) are the powers of the interfering core and cladding modes at wavelength λ, and L is the length of the HC-PCF. The transmission spectrum is directly related to the optical path difference φ which depends on the differential effective index Δn of the two modes. Dips in the transmission spectrum can be observed when the phase matching condition is satisfied [30]:

$$\varphi = \frac{2\pi\Delta nL}{\lambda} = \frac{2\pi(n_{co} - n_{cl})L}{\lambda} = (2n+1)\pi \tag{3.2}$$

where n is some positive integer and φ is the phase difference between the two interfering modes. $n_{co}$and n_{cl} denote the effective modal refractive indices of the fundamental core mode and the higher order cladding modes respectively.

Application of axial strain, or here, microstrain, results in the elongation in length of the PCF or, a transverse contraction of the PCF. Since, the phase difference between the two interfering modes depends on the length, L of the PCF as well as the effective index Δn between the modes, there occurs a shift in the resonance wavelength in the spectrum due to change in length of the HC-PCF. The resonance wavelength is given by [30]

$$\lambda = \frac{(n_{co} - n_{cl})L}{2n+1} \tag{3.3}$$

The shift in the resonance wavelength due to the change in the length of the fiber can be calculated by differentiating (3.3) with respect to L. This is given by [21], [37]

$$\Delta\lambda = 1 + \frac{L}{\Delta n}\frac{d(\Delta n)}{dL}\lambda \tag{3.4}$$

As can be seen from (3.4), the shift in resonance wavelength is a linear function of the strain applied. Thus, this shift can be employed for the measurement of applied strain.

In this chapter, we have investigated two different geometries of hollow core PCF as strain sensors. We call these as large core PCF and small core PCF. Both of these are hexagonal lattice structures designed with silica as the base material comprising of circular air holes centered on a hollow circular core. The parameters of the two fibers used in our investigation are listed in table 3.1.

Table 3.1 Parameters of HC-PCF

PARAMETER	LARGE-CORE PCF	SMALL-CORE PCF
Pitch, Λ	2 μm	7 μm
Air filling fraction , d/Λ	0.75	0.45

As can be seen from (3.4), the shift in resonance wavelength is higher at longer wavelengths [30], thus the operating wavelength is chosen as 1550 nm in order to achieve higher strain sensitivity. Different levels of strain ranging from 0 με to 2000 με are applied on both the structures (assuming uniform deformation of the holes through- out the structure), and the corresponding shift in resonance wavelength is observed. Strain sensitivities of both the sensor structures are calculated and compared. Effect of changes in SRI on the strain sensitivity of the said sensor is also analyzed.

3.3 RESULTS AND DISCUSSION

We analyzed the mentioned sensor geometries individually for different strain levels ranging up to 2000 με. Generally, micro level of strain induces minute changes in the length of the sensor as well as in its cross sectional geometry. This affects the position of the dips obtained in the spectrum, as compared to the condition when no strain was applied. By correlating the position of these dips in the spectrum, a calibration curve can be obtained. The transmission spectrum of small core HC-PCF, when it is subjected to four different levels of axial strain can be seen in fig. 3.1. A significant shift in the wavelength of the transmission dips is observed near wavelengths 1540 nm and 1560 nm.

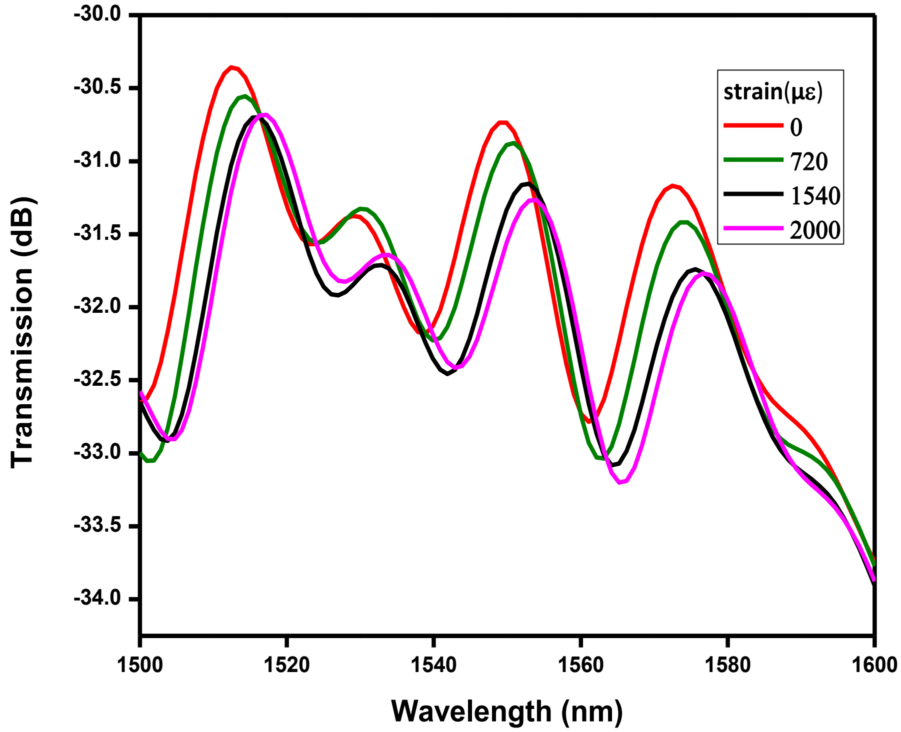

Fig.3.1 Transmission spectra of small core HC-PCF with different levels of applied strain

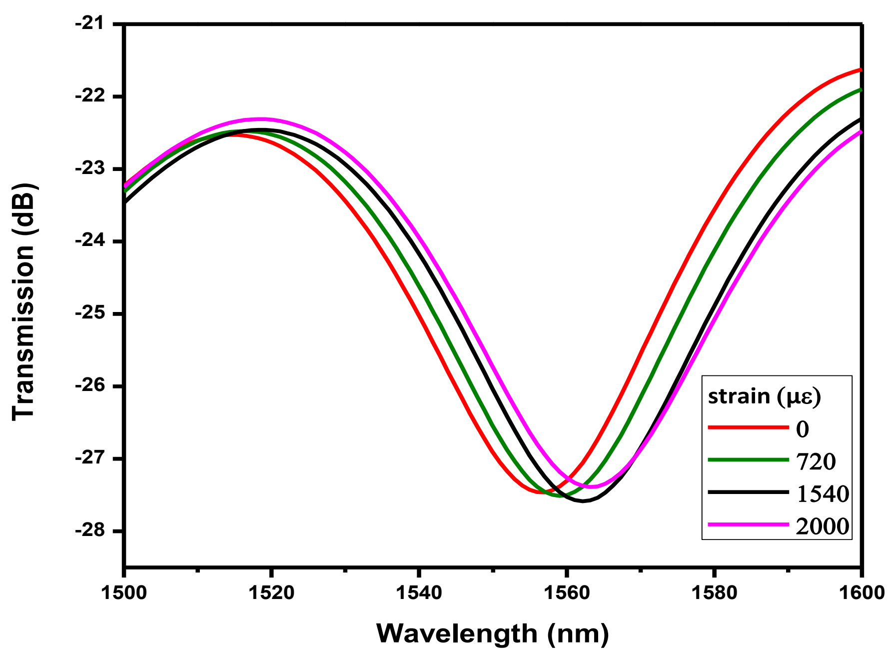

Fig. 3.2 Transmission spectra of large core HC-PCF with different levels of applied strain

We observe a similar shifting of the transmission spectrum around wavelength 1560 nm for the large core HC-PCF when subjected to varying strain levels as shown in fig. 3.2. Thus, the applied strain can be detected and evaluated by measuring the shift in the resonance wavelength. We observe from fig.3.1 and 3.2 that the transmission dips shift to a longer wavelength without a change in shape. Only a variation in intensity is observed which indicates participation of more than two modes in the process of interference [38].

The relationship between the wavelength of the dips and the applied strain for small core PCF and large core PCF geometries of the sensor are shown in fig. 3.3 (a) and (b), respectively. A linear behavior can be seen in both these cases. The value of correlation factor R^2=0.99717 and R^2= 0.99849 are obtained from fig. 3(a) and (b), respectively. The strain sensitivity of the said sensor can be calculated by measuring the slope of the wavelength shift versus strain curve. We obtained high strain sensitivities of 2.3 pm/με and 3.71 pm/με for small core HC-PCF and large core HC-PCF, respectively.

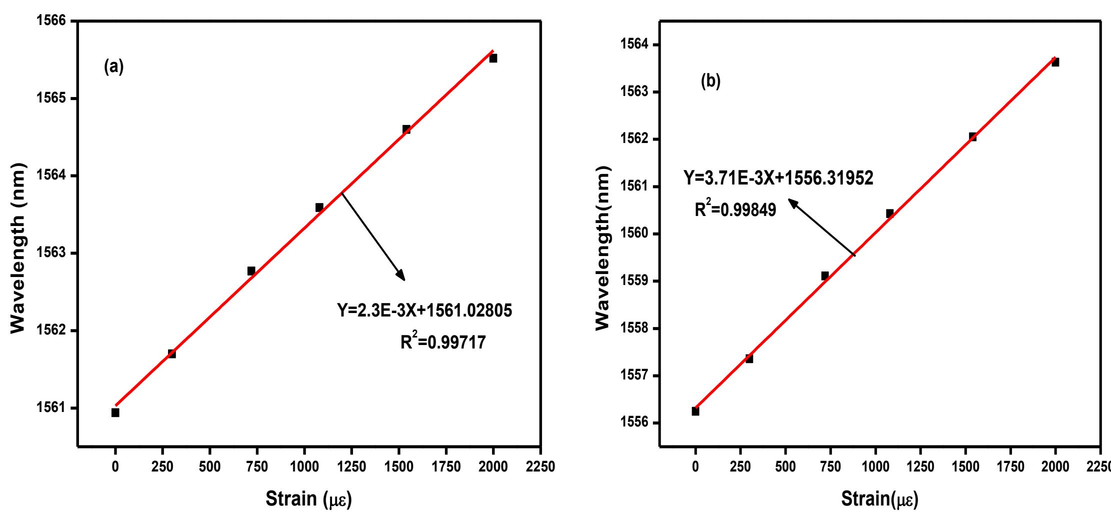

Fig. 3.3 Wavelength shift versus strain graph for (a) small core HC-PCF (b) large core HC-PCF

We observed that strain sensitivity achieved with large core HC-PCF is comparatively higher than that achieved with small core HC-PCF. This observation shows that lower pitch or, higher air filling fraction in a HC-PCF results in a greater sensitivity for strain. The sensitivity of large core HC-PCF, i.e., 3.71 pm/ με is also higher as compared to the earlier reported PCF based strain sensors. We also investigated the large core HC-PCF for variations in SRI. The dependence of resonance wavelength shift on changes in the refractive index of the surroundings is shown in fig.3.4.

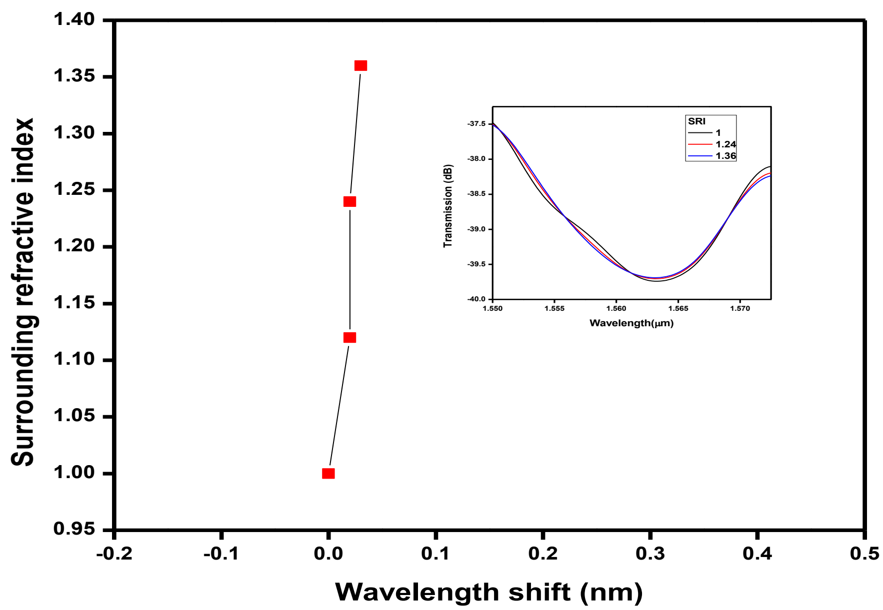

Fig. 3.4 Resonance wavelength dependence of large core HC-PCF on SRI (Inset: transmission spectra of large core PCF for different SRI as indicated)

We observe that the wavelength shift is negligible for variations in SRI, hence, the strain sensitivity for HC-PCF remains unaffected by refractive index changes in the environment. This property of HC-PCF makes it an attractive solution as a sensor for environments with variable refractive index.

3.4 CONCLUSION

This chapter has presented a simple configuration of hollow core PCF based strain sensor. A high strain sensitivity of 3.71 pm/με is observed with large core HC-PCF as compared to 2.3 pm/με with small core PCF signifying the role of higher air filling fraction in sensing. The strain sensitivity of 3.71 pm/με is also higher than the previously reported HC-PCF based strain sensors. The sensor shows linear response to strain and also, is independent of surrounding refractive index. Due to demonstrated sensitivity, the presented sensor is an attractive solution for applications such as strain measurement in hazardous environments and health monitoring of complex structures.

CHAPTER-4

RESPONSE TO STRAIN OF A METAL FILLED TWIN-CORE PCF FOR APPLICATION AS A MICRO-STRAIN SENSOR

Twin-core photonic crystal fiber consists of two solid cores separated by an air hole. We, in this chapter have investigated metal-filled TC-PCF as a micro-strain sensor. Using metal to separate two cores of the fiber results in stronger coupling and lower losses, as well as maintenance of the compact structure of PCF. TC-PCF based sensor exhibits a high sensitivity which is comparable to existing PCF-based sensor configurations. The dependence of sensitivity of the strain sensor on parameters of TC-PCF has been studied in this chapter.

4.1 INTRODUCTION

Fiber optic sensors have emerged as a unique solution in particular cases like potentially explosive environments or those with electrical hazard, etc. Although, conventional optical fiber-based sensors are well established [33], PCFs, despite of its youth in sensing field has gained attention of the researchers. PCF is a lately developed class of optical fiber [34] which are characterized by periodic arrangement of air-filled capillaries running along whole length of the fiber, centered on a hollow or solid core. Optical properties of air-silica PCFs can be altered by varying the location, shape and size of the air filled holes and can be extended by filling the holes with materials other than air, like liquid crystals [39], semiconductors [40], or metals [41], [42] etc., and as a result they prove advantageous for sensing applications. For the past few years, PCF-based surface plasmon resonance sensing is continuously being exploited in the fields of medical diagnostics, drug control and food control [43]. Such sensors utilize the phenomenon of coupling between the fundamental core mode and the plasmon mode. These offer several advantages, like miniaturization, an elevated degree of integration and remote sensing abilities.

With the development in the field of sensing, PCF-based SPR sensors have entered into the area of physical sensing as well. S. Jhang *et al.* [44] analyzed a PCF structure with hexagonal silver-coated air holes for pressure sensing applications and achieved a high value of sensitivity as 32.89 nm/N. Y. Peng *et al.* [45] had demonstrated a PCF-based SPR temperature sensor to obtain a temperature sensitivity of 720 pm/°C. Y. Lu *et al.* [46] reported a higher temperature sensitivity of 2.7 nm/°C by using dual function of analyte and silver wires to realize temperature sensing.

Use of twin-core PCFs (TC-PCF), where two solid cores spaced by air are placed adjacent to each other; as strain sensors have been reported [31] due to their large index contrast and vast design opportunities. However, a long coupling length of the fiber results in reduction of coupling efficiency and increase in the confinement loss of the designed sensor. Miniaturization of the device is also desirable to be used as a sensor, which is not possible with a long coupling length.

In this chapter, we have analyzed a structure which uses metal wire as a separation between the two cores of the TC-PCF, in order to enhance directional power transfer and demonstrated the application of such TC-PCF geometry as a micro-strain sensor. Filling of metal wire in the centre maintains the compact structure of the PCF and is simple to implement. The FDTD method is used to simulate operation of the said sensor at different strain levels. A comparison of strain sensitivities obtained by varying certain parameters of the TC-PCF has also been done.

This chapter is organized into four sections. Section 4.1 gives an overview of the paper. Section 4.2 explains the basic principle of strain sensing based on TC-PCF with a metal wire. It also describes the simulation set-up of TC-PCF based strain sensor. The section 4.3 gives the discussion of the results observed after the simulations. The section 4.4 gives the conclusion about utilizing TC-PCF with a metal wire for the purpose of strain sensing.

4.2 THEORY AND SIMULATION SETUP

A PCF is made up of two materials which have a high contrast of refractive index. Thus, it can be referred to as a 3D structure having a 2D refractive index distribution such that the light remains confined to the core. A TC-PCF consists of two cores, generally solid and made of fused silica, placed adjacent to each other with a air hole separating the two. These two fiber cores in the cross section of TC-PCF act as two independent waveguides inside a single TC-PCF structure, accompanying the phenomenon of mode coupling. The coupling length of the fiber cores in the TC-PCF varies for various structures of the TC-PCF. Twin-core fibers with small air filling fraction result in shorter coupling lengths (due to stronger mode coupling), however, also in larger confinement losses [47]. We have used a metal wire instead of the air hole to separate the two cores of the TC-PCF. It has been shown that resonant coupling between the surface plasmon modes supported by the metal wire and the fiber core-guided modes may be utilized to improve the performance of twin-core PCF through a one-order-of-magnitude decrease in coupling length and enhancement in coupling efficiency [48]. Also, this technique doesn't add much to the cost and area of the design, to be used as miniaturized sensor device.

With the help of supermode theory, power coupling can be explained by the interference between the fiber core-guided odd and even supermodes, denoted as o- and e-, respectively [48], with no contribution of higher order modes in intercore power transfer [49]. If constructive interference takes place, the maximum power occurs in one of the cores, and in case of destructive interference, it is transferred to the other core [48]. The coupling length (L_c) of the fiber can be said as the shortest length of the fiber which supports peak power transfer among the two cores, and varies inversely with the Re(n_{eff}) difference between the even and the odd supermode [50]:

$$L_c = \frac{\lambda}{2\times|n_{eff}^{e} - n_{eff}^{o}|} \tag{4.1}$$

where, n_{eff}^{e} and n_{eff}^{o} are the effective refractive indices of the even and odd supermodes respectively. A significant increase in the value of $\mathrm{Re}(n_{eff}^{e}) - \mathrm{Re}(n_{eff}^{o})$ is observed due to occurrence of the resonant coupling in the TC-PCF structure filled with metal wire as compared to the unfilled TC-PCF. Hence, reduction in coupling length is achieved, thereby, reducing the size of the sensor device. A dip in the intensity curve occurs at the resonance wavelength, λ_r, where coupling is the strongest, and the difference term $|\mathrm{Re}(n_{eff}^{e}) - \mathrm{Re}(n_{eff}^{o})|$ value is maximum [48].

In other words, we observe a dip in the transmission spectrum of the said sensor when the phase matching condition for the plasmon mode and the core guided mode is satisfied [51]:

$$\frac{2\pi L_0 \Delta n_{eo}}{\lambda} = (2n + 1)\pi \tag{4.2}$$

where, n is an integer, L_0 is the length of the fiber ($L_0 \geq L_c$) and Δn_{eo} is the differential effective index $|n_{eff}^{e} - n_{eff}^{o}|$ between the modes.

Application of axial strain, ε, results in the elongation in length of the TC-PCF or, a transverse contraction of the TC-PCF. Since, the phase difference between the two interfering modes depends on the length, L_0 of the PCF as well as the effective index, Δn_{eo} between the modes, there occurs a alteration in the resonance wavelength in the spectrum due to change in length of the TC-PCF. The resonance wavelength is given by [30]:

$$\lambda_r = \frac{\Delta n_{eo} . L_0}{2n+1} \tag{4.3}$$

The shift in λ_r due to the change in the length of the fiber can be calculated by differentiating (4.3) with respect to L. This is given by [21], [37]:

$$\Delta\lambda_r = 1 + \frac{L_0}{\Delta n_{eo}} \frac{d(\Delta n_{eo})}{dL_0} \lambda\varepsilon \tag{4.4}$$

As can be seen from (4.4), the shift in resonance wavelength is a linear function of the axial strain. Thus, this shift can be employed for the measurement of strain applied.

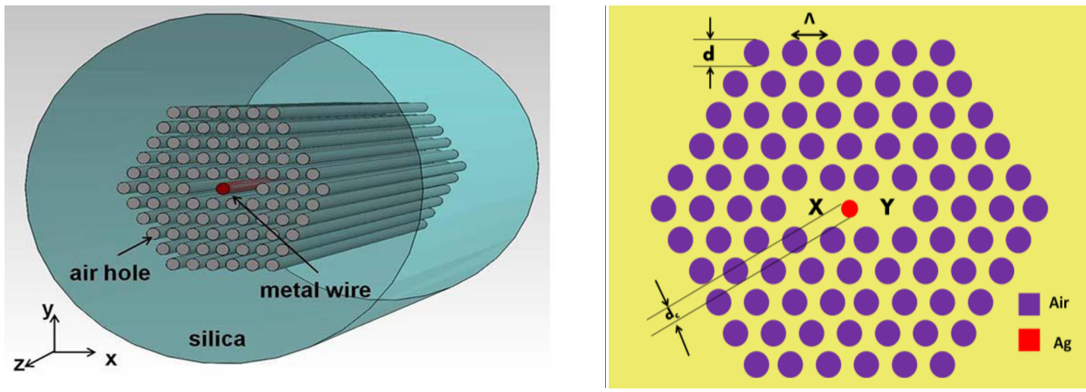

(a) (b)

Fig. 4.1 (a) Diagrammatic representation of TC-PCF geometry with metal wire inclusion in the center (red) (b) the layout model

In this chapter, we have numerically investigated a twin-core PCF structure including a metal wire (Ag) in the centre as a strain sensor. The geometry of the said sensor is shown in fig.4.1(a) with silver wire in the centre (marked as red). Selective filling of metal wire in central air hole can be realized with the use of pressure-assisted pumping [52], or femtosecond laser micromachining [53]. Fig.4.1(b) shows cross section of our simulation model, which is formed by a hexagonal array of air holes and with pitch, Λ = 2 μm, and air filling fraction, d/Λ= 0.75 (d is diameter of air holes). The two cores (X and Y), are separated by a circular hole filled with Ag wire, with diameter d_c=0.5 μm. The parameters of TC-PCF used in our investigation are summarized in table 4.1. We have assumed the refractive index of the air as 1.0 and that of fused silica is calculated as 1.444 at wavelength of 1550 nm with the help of Sellmeier equation [54]. The dielectric constant of Ag is described by the Drude model [55]. Different levels of strain ranging from 0 με to 2000 με are applied axially on the said structure (assuming uniform deformation of the holes throughout the structure), and the corresponding shift in resonance wavelength is observed. Strain sensitivity of the sensor structure is calculated and compared with those obtained by varying the parameters of TC-PCF to find out the optimum parameters for designing of the sensor.

Table 4.1 Parameters of Ag-filled TC-PCF

PARAMETER	VALUE
Pitch, Λ	2 μm
Air filling fraction , d/Λ	0.75
Diameter of Ag wire, d_c	0.5 μm

4.3 RESULTS AND DISCUSSION

We analyzed the TC-PCF sensor geometry for different strain levels ranging up to 2000 με. Generally, micro level of strain induces minute changes in the length of the sensor as well as in its cross sectional geometry. This affects the position of the dips obtained in the spectrum as compared to the condition when no strain was applied due to change in Δn_{eo}.

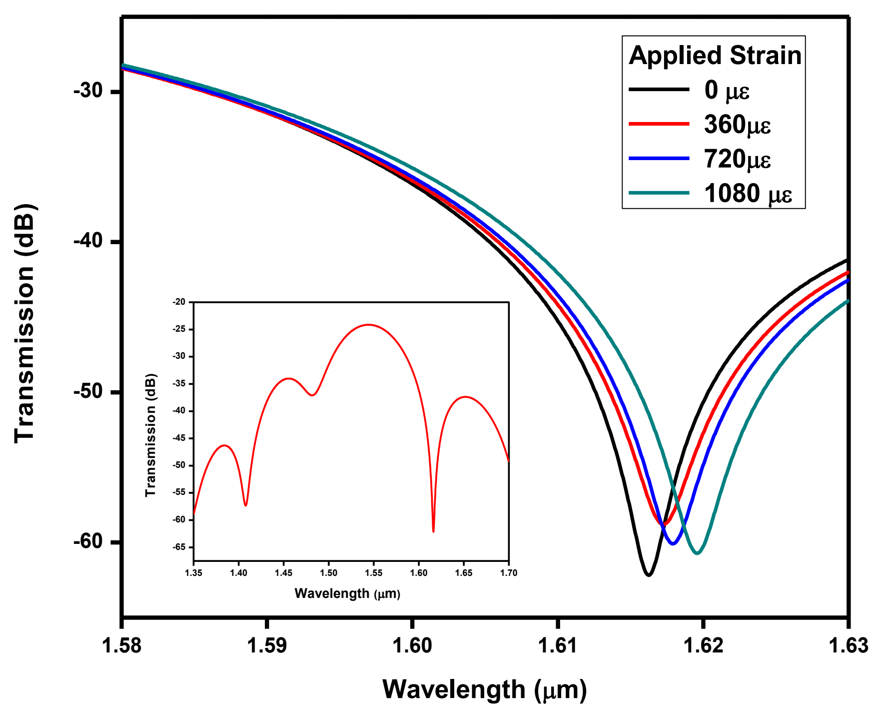

Fig. 4.2 Transmission spectra of TC-PCF filled with Ag wire at different levels of applied strain

By correlating the position of these dips in the spectrum, a calibration curve can be obtained. The transmission spectrum of TC-PCF filled with silver wire, when subjected to four different levels of axial strain can be seen in fig. 4.2. A significant shift in the wavelength of the transmission dips is observed near wavelength 1620 nm. The inset graph shows the transmission spectrum of the said sensor (when no strain is applied) in the range of 1380-1700 nm to obtain a detectable dip at 1616 nm.

The relationship between the wavelength of the dips and the applied strain for the TC-PCF geometry of the sensor is shown in fig. 4.3. A linear behavior can be seen in this case. The value of correlation factor R^2=0.99749 is obtained from fig. 4.3.

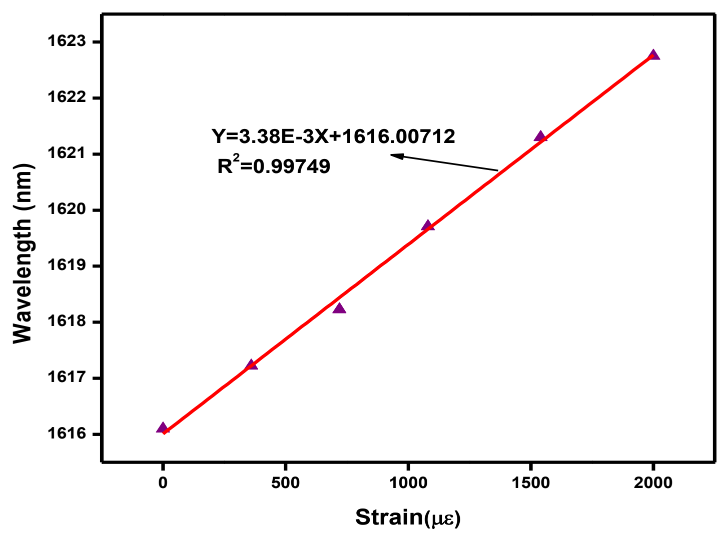

Fig 4.3 Wavelength shift versus strain graph for TC-PCF filled with Ag wire

The strain sensitivity of the said sensor can be calculated by measuring the slope of the wavelength shift versus strain curve. We obtained high strain sensitivity of 3.38 pm/με for the investigated design. The achieved sensitivity is higher as compared to the earlier reported PCF based strain sensors, and also the integration of SPR phenomenon in the design supports lower confinement losses as well as higher coupling efficiency [48].

The shift in the resonance wavelength with change in Λ values ranging from 2-2.4 μm at different values of applied strain is shown in fig. 4.4. The remaining parameters are kept fixed. We observe that a better shift is obtained at Λ =2 μm as compared to Λ =2.2 μm or

2.4 μm. Thus, we can say that Λ= 2 μm is the preferred value for the investigated structure.

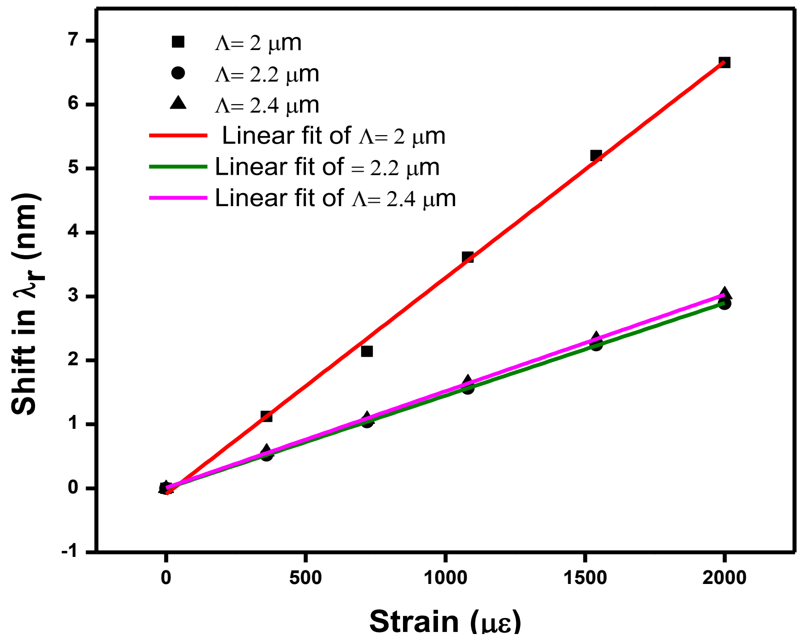

Fig. 4.4 Effect of Λ on resonance wavelength of TC-PCF structure at different levels of strain

We again compared the resonance wavelength shift of the said sensor for variation in d_c (0.45-0.55 μm) with Λ and d/ Λ fixed at 2 μm and 0.75 respectively.

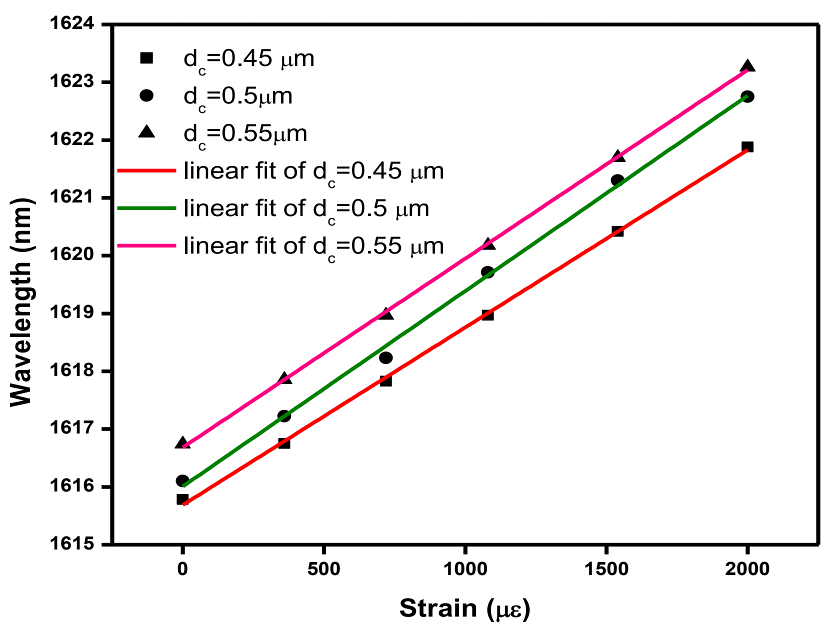

Fig. 4.5 Effect of d_c on resonance wavelength of TC-PCF structure at different levels of strain

As can be observed from fig.4.5, all the values of d_c gives a linear curve with respect to applied strain. Comparing the slopes, we get a higher slope, or a better sensitivity for d_c = 0.5 µm. Hence, this value is preferred for carrying out the simulations. The said sensor showed linear behavior only, when we varied the air filling fraction of the design from 0.75 to 0.7 and 0.8 (fig.4.6). Although, a decrease in slope is observed as compared to d/ Λ = 0.75. Hence, this value is chosen, in order to achieve a higher strain sensitivity with the TC-PCF sensor design.

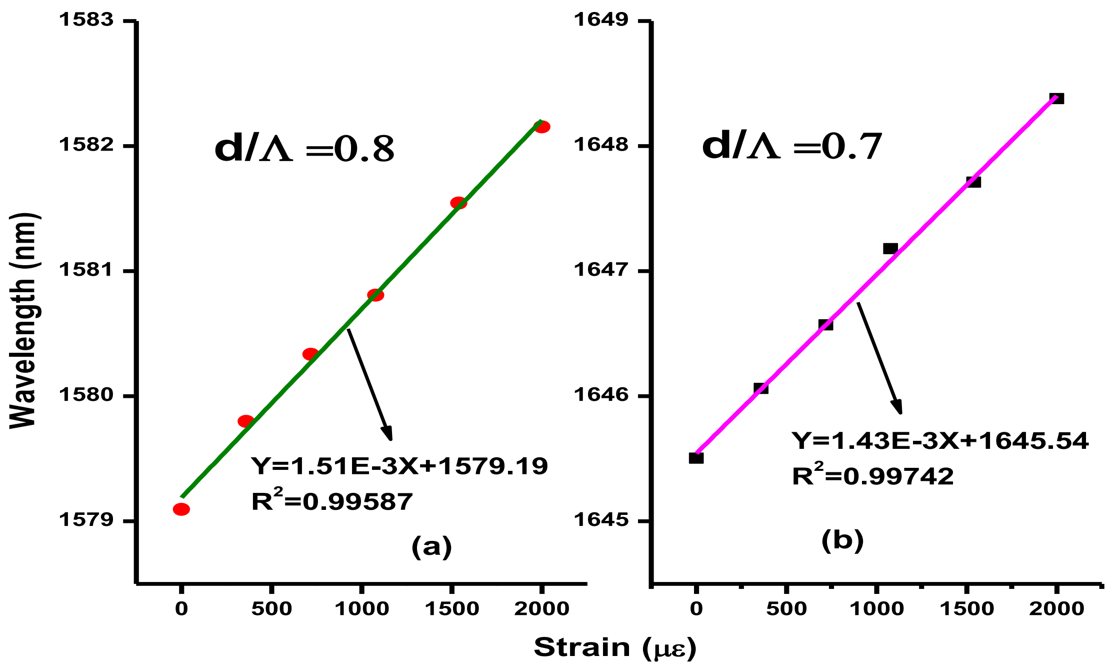

Fig. 4.6 Graph of shift in resonance wavelength versus strain; Λ=2 µm, d_c=0.5 µm (a) d/ Λ =0.8 (b) d/ Λ =0.7

Metal inclusion configuration is chosen to be a metal wire, as this design outperforms the rest configurations, i.e., metal layer, metal tube or a metal hole in terms of performance indicators like coupling efficiency, extinction ratio, confinement loss etc. [48]. Also, fabrication of metal wires is easier to realize as compared to other geometries.

4.4 CONCLUSION

A simple configuration of strain sensor based on twin core PCF structure with a central metal wire inclusion has been presented in this chapter. A linear response to strain and a high strain sensitivity of 3.38 pm/με are observed which is comparable to existing configurations of PCF-based sensors. Additionally, inclusion of the metal wire has a benefit of increase in coupling efficiency of the fiber as well as lowering the confinement losses. We also observed that the application of micro-strain results in shifting of the transmission spectrum towards longer wavelengths. This shifting is also dependant on the diameter of the metal wire used in the centre (d_c) as well as Λ and d/Λ of the TC-PCF structure. Due to demonstrated sensitivity, and high coupling efficiency, the presented sensor is an enhanced solution for applications such as measurement of strain in hazardous environments and health monitoring of civil structures. Also, the investigated structure is compact and easier to fabricate as compared to other metal inclusion configurations known till date.

CHAPTER-5

SENSITIVITY-ENHANCED MICRO-STRAIN SENSOR BASED ON BIREFRINGENT GERMANIUM DOPED HYBRID PCF

Hybrid PCF is formed by replacing one row of air holes in regular PCF with high-index Ge-doped silica rods so as to introduce natural birefringence in the fiber. In HPCF, light is guided simultaneously via two propagation mechanisms: modified total internal reflection and photonic bandgap guiding. In this chapter, we have investigated application of HPCF with Ge-doped inclusions as a micro-strain sensor. High birefringence of HPCF contributes in enhancement of sensitivity of the sensor as well as solves the problem of light polarization control, encountered with other optical fiber sensors. The dependence of sensitivity of the strain sensor on parameters of HPCF has been studied in this chapter.

5.1 INTRODUCTION

Photonic Crystal Fibers (PCFs) are a sub-division of optical fibers [34] which are characterized by periodic arrangement of air-filled capillaries along entire length of the fiber, centered on a solid or hollow core. In general, PCFs exhibit two mechanisms for guidance of light through the fiber: PBG and mTIR, depending on the geometry of the PCF and selection of core/ cladding materials [6]. Although, in case of HPCF, light is guided simultaneously via both the propagation mechanisms: mTIR from an array of air holes and PBG guiding due to inclusion of a high-index material [14]. The biggest attraction in PCFs is that by variation of the geometry of the holes of the cladding and/or the core, the transmission spectrum, dispersion, birefringence etc. such values can be reached, which are not possible with standard optical fibers. PCFs turn out to be a promising and enhanced solution for practical applications where monitoring of strain-induced variations is essential, such as, in the fields of experimental mechanics, metallurgy, aeronautics, and significantly, in health monitoring of complex structures [4].

Y.G. Han *et al.* [56] investigated simultaneous strain and temperature measurement with help of a simple configuration of temperature insensitive birefringent interferometer utilizing erbium-doped PCF and attained high strain and temperature sensitivities of 1.3 pm/με and -0.04 dB/°C respectively. B. Gu *et al.* [57] presented an interferometric strain and temperature sensor based on all-solid birefringent HPCF to achieve higher values of strain and temperature sensitivities as 23.8 pm/με and 1.12 nm/°C. G. S. Barabach *et al.* [58] reported a compact in-line fiber interferometric temperature and strain sensor using boron-doped PCF to overcome typical drawbacks of PCF-based interferometric sensors. High strain sensitivity of -2.51 nm/mstrain and thermal sensitivity of 16.7 pm/°C were reported with the presented configuration.

In standard PCF-based interferometers used for the purpose of sensing, it is difficult to control the polarization of the light. Hybrid PCFs possess a high birefringence which aids in overcoming this difficulty. Also, due to large value of birefringence, separate intermodal fringes are produced by each pair of polarization modes, resulting in contrast modulation of the output signal. Thus, simultaneous measurement of two different physical parameters is possible with the help of HPCFs [48].

In this chapter, we have presented a HPCF structure with inclusions of a high-index material (Ge-doped Silica) along one axis of the PCF with solid silica core, making the fiber naturally birefringent. The application of such HPCF geometry for measurement of strain has been demonstrated. The FDTD method is used to simulate operation of the said sensor at different strain levels. A comparison of strain sensitivities obtained by varying certain parameters of the HPCF has also been done.

This chapter is organized into four sections. Section 5.1 gives an overview of the paper. Section 5.2 explains the basic principle of strain sensing based on HPCF with Ge-doped inclusions. It also describes the simulation set-up of HPCF based strain sensor. The section 5.3 gives the discussion of the results observed after the simulations. The section

5.4 gives the conclusion about utilizing HPCF with Ge-doped inclusions for the purpose of strain sensing.

5.2 THEORY AND SIMULATION SETUP

A PCF is made up of two materials which have a high contrast of refractive index. Thus, it can be referred to as a 3D structure with 2D refractive index distribution such that the light remains confined to the core. A hybrid PCF structure consists of a hexagonal array of air holes centered on a solid core made up of undoped silica, with one layer of air holes replaced by high-index rods [14] as shown in fig.5.1(a). Along the y-axis, phenomenon of mTIR takes place, similar to of index-guiding PCFs, as a consequence of core having higher refractive index than the cladding effective refractive index. In contrast, TIR is not possible along the x-axis, since refractive index of the cladding rods is higher than the core. Thus, light is confined only in restricted bands of wavelength, which overlap with the photonic bandgaps, occuring at the antiresonant conditions of the high-index inclusions [14].

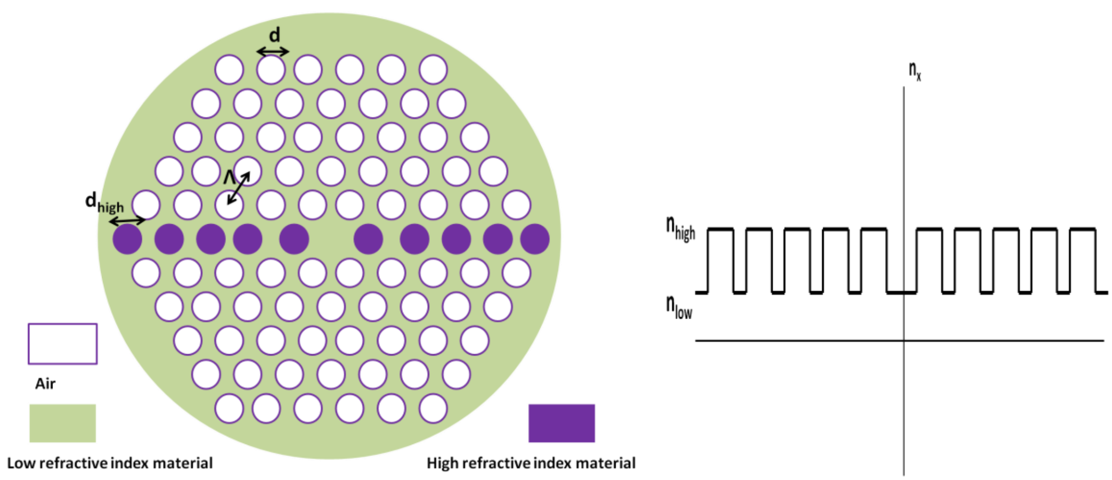

Fig.5.1 (a) Layout structure of HPCF; Λ-pitch of fiber, d- diameter of air holes, d_{high}- diameter of high-index inserts (b) Variation of refractive index of HPCF along x-axis

Fig.5.1(b) shows the effective index distribution of the HPCF. The inclusion of high-index rods along one axis of the PCF introduce birefringence in the fiber. Thus, it is possible to achieve PBG guiding and birefringence simultaneously in HPCFs. Although, light is guided through fiber by PBG and mTIR simultaneously, properties affected by photonic bandgap remain conserved [57].

The photonic bandgap in a fiber exhibits a sensitive nature towards external disturbances, like temperature, strain and curvature [57]. This nominates HPCFs as a suitable candidate to be utilized for the sensing purposes as they offer high birefringence and low losses also, in addition to hybrid guidance mechanisms. When light enters a HPCF, a relative phase difference is introduced between the two orthogonal guided modes due to high birefringence of HPCF, and its transmission spectrum can be expressed as [59], [60]:

$$t = \frac{1}{2} A_0(\lambda)[1 - \cos\phi] \tag{5.1}$$

$$\phi = \frac{2\pi}{\lambda}. K. L \tag{5.2}$$

$$K = n_{eff}^{y} - n_{eff}^{x} \tag{5.3}$$

where, $A_0(\lambda)$ defines intensity spectrum of HPCF due to PBG guidance effect, ϕ is the relative phase difference introduced between the orthogonal interfering modes, K is the birefringence introduced due to high-index inserts, λ is the operating wavelength and L is the length of HPCF. n_{eff}^{y} and n_{eff}^{x} denote the effective refractive indices of the x- and y-polarized modes of the HPCF, respectively.

A dip in the transmission spectrum is observed when the phase matching condition of the two orthogonal guided modes is satisfied [23]:

$$\phi = \frac{2\pi(n_{eff}^{y} - n_{eff}^{x})L}{\lambda} = (2n + 1)\pi \tag{5.4}$$

where, n is an integer.

Application of axial strain, $\varepsilon = \Delta L/L$ results in the elongation in the length of HPCF, or a transverse contraction of the HPCF; ΔL is the amount of longitudinal elongation of the fiber. The applied strain also causes the birefringence to change its value. Thus, there occurs a change in the relative phase difference present between the interfering orthogonal modes, as it depends on length, L of the HPCF as well as the birefringence, K of the fiber. The change in relative phase difference, $\Delta\phi$, is given as [57]:

$$\Delta\phi = \frac{2\pi\,(L.\Delta K + K.\Delta L)}{\lambda} \tag{5.5}$$

where, ΔK is the amount of variation in the birefringence of HPCF due to applied strain. This, in turn, modifies the phase matching condition stated in (5.4) to shift the dip wavelength of the transmission spectrum. Thus, the shift in the dip wavelength can be employed for interrogation of applied strain on the fiber.

In this chapter, we have numerically investigated a hybrid PCF structure with Ge-doped inclusions as a strain sensor. The cross section of the hybrid PCF is shown in fig.5.1(a), which is created by hexagonal arrangement of air holes with air filling fraction, $d/\Lambda = 5/9$ around undoped silica core and central row of air holes is substituted by Ge-doped silica inclusions. The GeO_2 concentration in the inclusion is 15 mol%. We have assumed the refractive index of the air as 1.0 and that of fused silica is calculated as 1.444 at wavelength of 1550 nm with the help of Sellmeier equation [54]. The refractive index of Ge-doped inserts is calculated as [61]:

$$N_{dop} = (1 - X_{mol}).\,N_{SiO_2} + X_{mol}.\,N_{GeO_2} \tag{5.6}$$

where, N_{dop} is the refractive index of Ge-doped silica inclusions, X_{mol} indicates molar concentration of GeO_2 in doped silica and N denotes refractive indices of SiO_2 or GeO_2 at a particular wavelength. The parameters of HPCF used in our investigation are summarized in table 5.1.

Table 5.1 Parameters of Ge-doped HPCF

PARAMETER	VALUE
Air filling fraction , d/Λ	5/9
Ratio of diameters of air holes to Ge-doped inserts, d/D	2/3
Concentration of GeO_2 in doped silica, X_{mol}	15 %

Different levels of strain ranging from 0 με to 2000 με are applied axially on the said structure (assuming uniform deformation of the holes throughout the structure), and the corresponding shift in resonance wavelength is observed. Two different structures of hybrid PCF are analyzed for d/D<1 and d/D>1 and respective strain sensitivities are compared. A comparison of strain sensitivities obtained by variation of parameters like X_{mol}, d/Λ and d/D has also been done.

5.3 RESULTS AND DISCUSSION

We analyzed the HPCF sensor geometry (d/D=2/3) for different strain levels ranging up to 2000 με. Generally, micro level of strain induces minute changes in the length of the sensor as well as in its cross sectional geometry. This affects the position of the dips obtained in the spectrum as compared to the condition when no strain was applied due to change in birefringence. By correlating the position of these dips in the spectrum, a calibration curve can be obtained. Fig. 5.2 shows the transmission spectrum of HPCF with Ge-doped inclusions (when no strain is applied) in the range of 1480-1650 nm to obtain a detectable dip at 1590 nm.

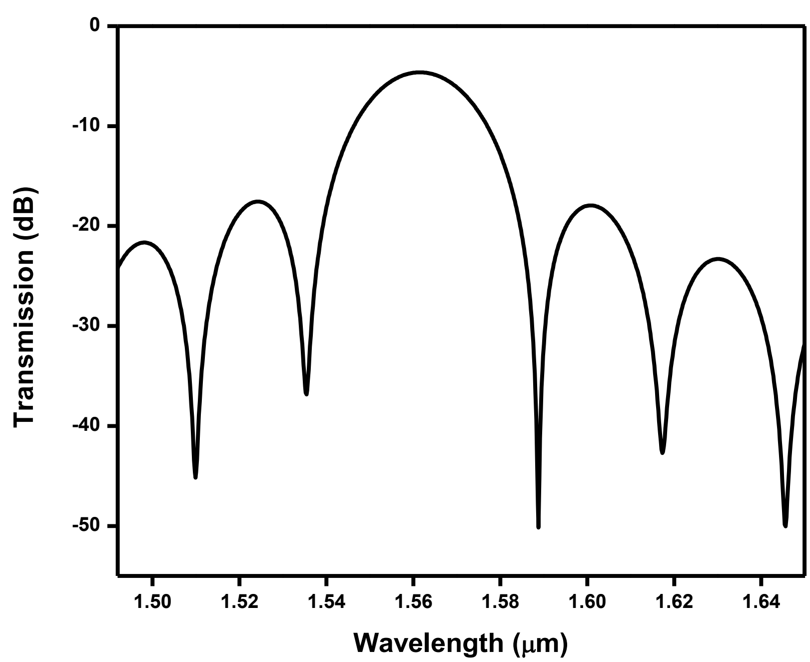

Fig. 5.2 Transmission spectrum of HPCF with Ge-doped inserts without application of strain

The transmission spectrum of said sensor, when subjected to different levels of axial strain can be seen in fig. 5.3. The wavelength of the transmission dips is considerably shifted towards shorter wavelengths accompanied with a decrease in transmission intensity.

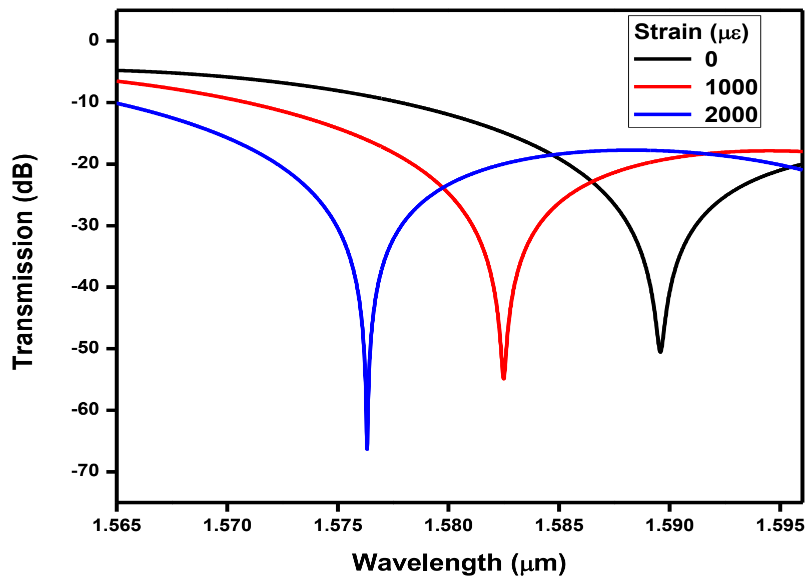

Fig. 5.3 Transmission spectra of HPCF with Ge-doped inserts at different levels of applied strain

The relationship between the wavelength of the dips and their observed intensity levels with applied strain for the HPCF geometry of the sensor is shown in fig. 5.4.

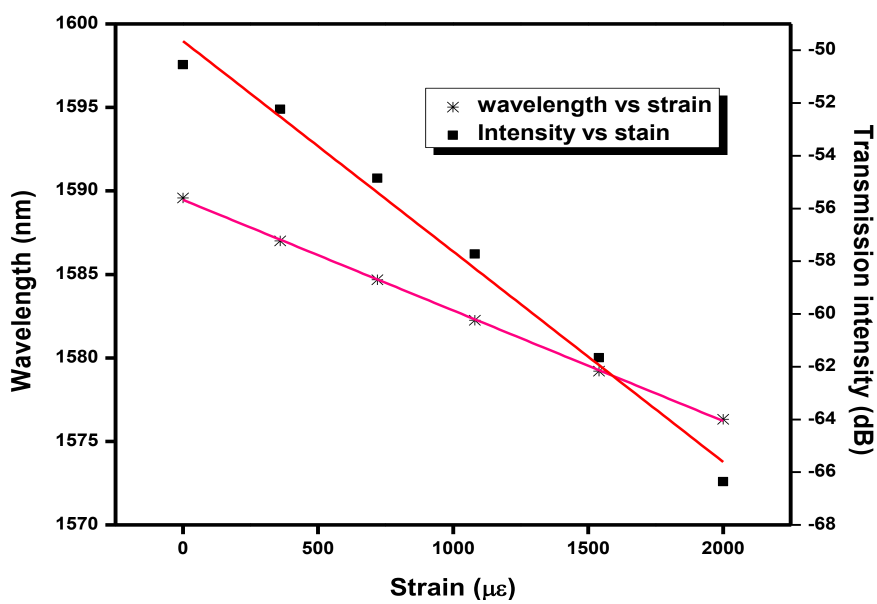

Fig. 5.4 Wavelength shift/ transmission intensity versus strain graph for HPCF with Ge-doped inclusions

A linear behavior can be seen in the investigated range, for both the cases. The value of correlation factor R^2=0.99962 and R^2=0.9853 is obtained for wavelength based interrogation and intensity based interrogation, respectively, from fig. 5.4. The strain sensitivity of the said sensor can be calculated by measuring the slope of the wavelength shift/ intensity versus strain curve. We obtained high strain sensitivity of -6.62 pm/με for the wavelength based interrogation of the investigated design. We also observed that the transmission intensity decreases at a rate of -7.98 dB/ με. The achieved sensitivity is higher as compared to the earlier reported PCF based strain sensors. Also, HPCF geometry contributes for maintenance of light polarization due to their high birefringence.

We also measured the shift in resonance wavelength with applied strain at different concentrations of GeO_2 in doped silica and computed the corresponding sensitivities as shown in fig. 5.5.

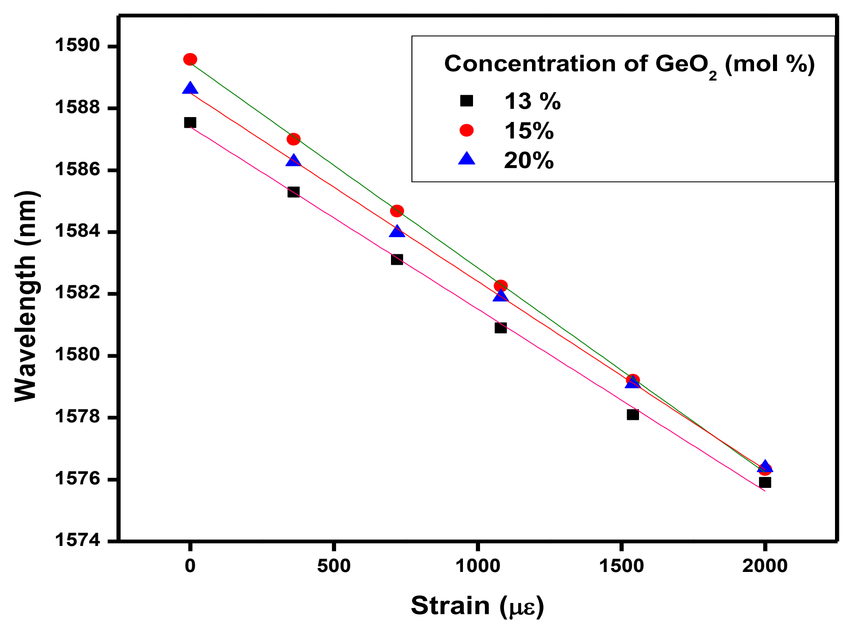

Fig. 5.5 Effect of X_{mol} on resonance wavelength of HPCF with Ge-doped inclusions

We obtained the values of strain sensitivity as -5.89pm/με, -6.62 pm/με and 6.09 pm/με at X_{mol}= 13%, 15% and 20% respectively. The remaining parameters are kept fixed at d/D=2/3 and d/Λ=5/9. Thus, we carried out rest of our simulations for X_{mol}=15% as it gives a higher value of strain sensitivity. We also analyzed a different geometry of HPCF with d/D=3/2 and achieved a lower sensitivity of -1.09 pm/με as shown in fig. 5.6. Hence, we can say that d/D<1 should be preferred for the investigated structure.

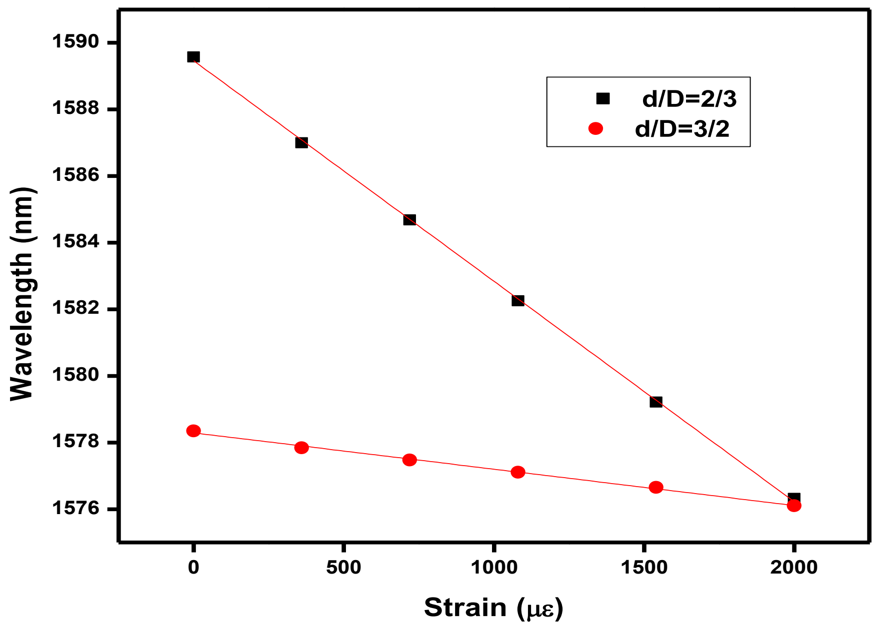

Fig. 5.6 Comparison of sensitivity of HPCF with Ge-doped inclusions for d/D>1 and d/D<1

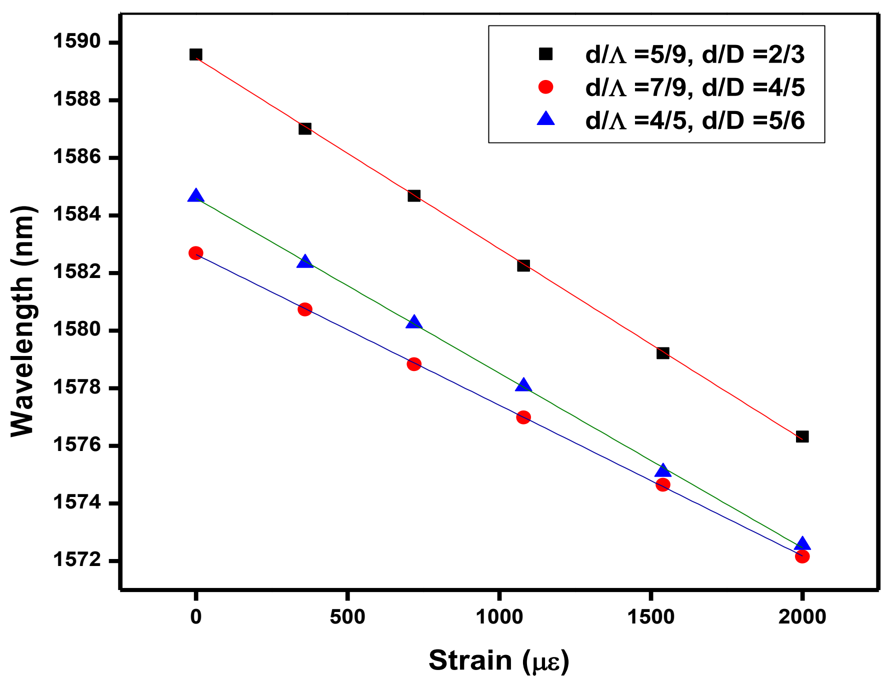

Fig. 5.7 Effect of d/D and d/ Λ on resonance wavelength of HPCF with Ge-doped inclusions

We examined the behavior of the said sensor for variation in other parameters while keeping X_{mol} fixed at 15% and d/D<1 as shown in fig. 5.7. It can be observed from the figure that all the values of d/D and d/Λ give a linear curve with respect to the applied strain. Strain sensitivity of -5.23 pm/με is achieved with d/Λ=7/9 and d/D=4/5 while a sensitivity of -6.06 pm/με is attained with d/Λ=4/5 and d/D=5/6. Thus, a decrease in slope is observed from what we achieved with d/Λ=5/9 and d/D=2/3. Hence, these values are selected, in order to achieve a better strain sensitivity with HPCF sensor design.

5.4 CONCLUSION

A simple configuration of strain sensor based on hybrid PCF structure with Ge-doped inclusions in the central row has been presented in this chapter. A linear response to applied strain and high strain sensitivities of -6.62 pm/με and -7.98 dB/με are observed with wavelength and intensity based interrogations respectively. Additionally, high birefringence of HPCF contributes to controlling of light polarization. We also observed that the application of micro-strain results in shifting of the transmission spectrum towards shorter wavelengths. The shifting is also dependant on concentration of GeO_2 in doped silica (X_{mol}), as well as d/D and d/Λ of the HPCF structure. Due to demonstrated sensitivity, and low losses in HPCF, the presented sensor is an enhanced solution for applications such as measurement of strain in hazardous conditions and health monitoring of complex structures.

CHAPTER-6

CONCLUSION, RECOMMENDATIONS AND FUTURE SCOPE

This chapter provides the summary of research work done in this dissertation. Firstly, the conclusions have been made from this study, then the recommendations have been given on the basis of the conclusions and after that suggestions for future research are discussed.

6.1 CONCLUSION

The major results obtained in this dissertation are summarized below:

1. A simple configuration of hollow core PCF based strain sensor has been presented. Observed sensitivity is almost double the value of that achieved with typical FBG-based sensors and higher than previously reported HC-PCF based sensor configurations. A high strain sensitivity of 3.71 pm/με is observed with large core HC-PCF as compared to 2.3 pm/με with small core PCF signifying the role of higher air filling fraction in sensing. The sensor shows linear response to strain and also, is independent of surrounding refractive index. Thus, the presented sensor is an attractive solution for applications such as strain measurement in environments with varying refractive index and health monitoring of complex structures.
2. A simple configuration of strain sensor based on twin core PCF structure with a central metal wire inclusion has been presented. A linear response to strain and a high strain sensitivity of 3.38 pm/με is observed which is comparable to existing configurations of PCF-based sensors. Additionally, inclusion of the metal wire has a benefit of increase in coupling efficiency of the fiber as well as lowering the confinement losses. The investigated structure is compact (due to short coupling length) and easier to fabricate as compared to other metal inclusion configurations

known till date. Thus, the presented sensor has a great potential for strain monitoring applications to sense even very minute levels of strain with low losses.

3. A simple configuration of strain sensor based on hybrid PCF structure with Ge-doped inclusions in the central row has been presented. Both wavelength and intensity based interrogations are carried out to observe a linear response to applied strain and high strain sensitivities of -6.62 pm/με and -7.98 dB/με respectively. The achieved sensitivity is enhanced in comparison to regular PCF-based sensors due to high natural birefringence of HPCF and low losses. Due to demonstrated sensitivity, and low losses in HPCF, the presented sensor is an enhanced solution for strain monitoring in all such applications where changes due to external parameters like displacement, vibration etc. can be transformed into strain induced changes.

6.2 RECOMMENDATIONS

Based on the above conclusions, some recommendations have been made:

HC-PCF based strain sensors prove better than the conventional FBG-based fiber optic strain sensors due to higher sensitivity to strain and offer stability to changes in SRI, thus they can be used in sensing applications which require a cost effective and miniaturised system and a trade off between sensitivity and losses is feasible.

Metal-filled TC-PCF based strain sensors exhibit a high sensitivity as well as low coupling losses, although, inclusion of metal increases the overall cost of the sensor. Thus, it can be used for strain monitoring applications where precision is a more important factor than the cost of the sensor, such as health monitoring of civil structures.

HPCF based strain sensors result in an enhanced sensitivity as well as low losses, although, they do not completely eliminate sensitivity to other parameters. Thus, they find use in strain sensing applications where cross sensitivity is not a major issue, like sensing of strain in normal environments.

6.3 FUTURE SCOPE

During the course of this dissertation, several avenues for continuation of this study became evident. The topics which were considered worthwhile are summarized below:

In this dissertation, an index insensitive strain sensor based on HC-PCF has been studied. The analysis can be extended to make it insensitive to other parameters as well, like temperature, vibration etc. to observe a better performance in external environment.

We have considered Ag-metal for filling of the TC-PCF. Other metals/ alloys can be used for this purpose and results can be observed for a better sensitivity to strain and lower losses.

The cross-sensitivity of HPCF to external parameters has been neglected, assuming its function under normal environmental conditions. Simulation studies can be done with the same configuration taking into account temperature variations.

We have considered the operation of investigated sensors at wavelength of 1550 nm. Their operation can be simulated at other wavelengths also and results can be compared.

Sensitivity to axial strain has been considered in this dissertation. We can improve our designs so as to sense the transverse and axial strain separately, which is a major requirement in cure cycle monitoring of health structures.

REFERENCES

[1] F. Mitschke, Fiber optics: physics and technology, Heidelberg, New York: Springer, 2009.

[2] K. T. V. Grattan and T. Sun, "Fiber optic sensor technology: an overview," *Sensors and Actuators A,* vol. 82, no. 1, pp. 40-61, 2000.

[3] G. Rajan, "Introduction to optical fiber sensors," in *Optical fiber sensors: advanced techniques and applications*, CRC press, 2015, pp. 1-12.

[4] A. R. Pinto and M. Lopez-Amo, "Photonic crystal fibers for sensing applications," *Journal of Sensors,* vol. 2012, pp. 1-21, 2012.

[5] B. Troia, A. Paolicelli, F. D. Leonardis and V. M. N. Passaro, "Photonic crystals for optical sensing: a review," in *Advances in Photonic Crystals*, InTech, 2013, pp. 241-295.

[6] S. A. Cerqueira, "Recent progress and novel applications of photonic crystal fibers," *Reports on Progress in Physics,* vol. 73, no. 2, pp. 1-21, 2010.

[7] T. A. Birks, J. C. Knight and P. S. Russell, "Endlessly single mode photonic crystal fiber," *Optics Letters,* vol. 22, no. 13, pp. 961-963, 1997.

[8] N. A. Mortensen, J. R. Folkenberg, M. D. Nielsen and K. P. Hansen, "Modal cutoff and the V parameter in photonic crystal fibers," *Optics Letters,* vol. 28, no. 20, pp. 1879-1881, 2003.

[9] J. C. Knight, T. A. Birks, P. S. J. Russell and J. P. de Sandro, "Properties of photonic crystal fiber and the effective index model," *Journal of the Optical Society of America A: Optics Image Science and Vision,* vol. 15, no. 3, pp. 748-752, 1998.

[10] F. Luan, A. K. George, T. D. Hedley, G. J. Pearce, D. M. Bird, J. C. Knight and P. S. J. Russell, "All-solid photonic bandgap fiber," *Optics Letters,* vol. 29, no. 20, pp. 2369-2371, 2004.

[11] N. Litchinitser, S. Dunn, P. Steinvurzel, B. Eggleton, T. White, R. McPhedran and C. de Sterke, "Application of an ARROW model for designing tunable photonic devices," *Optics Express*, vol. 12, no. 8, pp. 1540-1550, 2004.

[12] J. C. Knight, F. Luan, G. J. Pearce, A. Wang, T. A. Birks and D. M. Bird, "Solid photonic bandgap fibers and applications," *Japanese Journal of Applied Physics*, vol. 45, no. 8A, pp. 6059-6063, 2006.

[13] S. Johnson, S. Fan, P. R. Villeneuve, J. Joannopoulos and L. A. Kolodziejski, "Guided modes in photonic crystal slabs," *Physical Review B,* vol. 60, no. 8, pp. 5751-5758, 1999.

[14] S. A. Cerqueira Jr., F. Luan, C. M. B. Cordeiro, A. K. George and J. C. Knight, "Hybrid photonic crystal fiber," *Optics Express*, vol. 14, no. 2, pp. 926-931, 2006.

[15] A. Taflove and S. C. Hagness, "Introduction to Maxwell's equations and Yee algorithm," in *Computational Electrodynamics: The Finite-Difference Time Domain Method*, Boston, Artech House, 2005, pp. 59-80.

[16] B. Culshaw, "Fiber optics in sensing and measurement," *IEEE Journal on Selected Topics in Quantum Electronics,* vol. 6, no. 6, pp. 1014-1021, 2000.

[17] N. H. M. Kamrujjaman Serker, "Structural health monitoring using static and dynamic strain data from long-gage distributed FBG sensor," in *IABSE-JSCE Joint Confrence on Advances in Bridge Engineering-II*, Dhaka, Bangladesh, 2010.

[18] A. Kesawan, S. John and I. Herszberg, "Strain-based structural health monitoring of complex composite structures," *Structural Health Monitoring,* vol. 7, no. 3, pp. 203-213, 2008.

[19] C. Sonnenfeld, G. Luyckx, F. Collombet, Y.-H. Grunevald, B. Douchin, L. Crouzeix, M. Torres, T. Geernaert, S. Sulejmani, K. Chah, P. T. H. Mergo and F. Berghmans, "Cure cycle monitoring of laminated carbon fiber-reinforced plastic with fiber bragg gratings in microstructured optical fiber," in *The 19th International Conference on Composite Materials,* Montreal, Canada, 2013.

[20] J. Villatoro, V. P. Minkovich and D. Monzon-Hemandez, "Temperature-independent strain sensor made from tapered holey optical fiber," *Optics letters,* vol. 31, no. 3, pp. 305-307, 2006.

[21] J. Villatoro, V. Finazzi, V. P. Minkovich, P. V. and G. Badenes, "Temperature-insensitive photonic crystal fiber interferometer for absolute strain sensing," *Applied Physics Letters,* vol. 91, no. 9, pp. 1-3, 2007.

[22] O. Frazao, J. M. Baptista and J. L. Santos, "Temperature independent strain sensor based on a Hi-Bi photonic crystal fiber loop mirror," *IEEE Sensors Journal,* vol. 7, no. 10, pp. 1453-1455, 2007.

[23] Q. Shi, F.Lv, Z.Wang, L.Jin, Z. J.J. Hu, G.Kai and X.Dong, "Environmentally stable Fabry-Perot-type strain sensor based on hollow-core photonic bandgap fiber," *IEEE Photonics Technology Letters,* vol. 20, no. 4, pp. 237-239, 2008.

[24] Y. G. Han, "Temperature-insensitive strain measurement using a birefringent interferometer based on a polarization maintaining photonic crystal fiber," *Applied Physics B,* vol. 95, no. 2, pp. 383-387, 2009.

[25] W. Qian, C. L. Zhao, X. Dong and W. Jin, "Intensity measurement based temperature-independent strain sensor using a highly birefringent photonic crystal fiber loop mirror," *Optics Communications,* vol. 283, no. 24, pp. 5250-5254, 2010.

[26] W. Zhou, W. C. Wong, C. C. Chan, L. Y. Shao and X. Dong, "Highly sensitive fiber loop ringdown strain sensor using photonic crystal fiber interferometer," *Applied Optics,* vol. 50, no. 19, pp. 3087-3092, 2011.

[27] L. M. Hu, C. C. Chan, X. Y. Dong, Y. P. Wang, P. Zu, W. C. Wong, W. W. Qian and T. Li, "Photonic crystal fiber strain sensor based on modified Mach-Zehnder interferometer," *IEEE Photonics Journal,* vol. 4, no. 1, pp. 114-118, 2012.

[28] W. Peng, X. Zhang, Z. Gong and Y. Liu, "Miniature fiber-optic strain sensor based on a hybrid interferometric structure," *IEEE Photonics Technology Letters,* vol. 25, no. 24, pp. 2385-2388, 2013.

[29] S. Rota-Rodrigo, A. M. R. Pinto, M. Bravo and M. Lopez-Amo, "An in-reflection strain sensing head based on a Hi-Bi photonic crystal fiber," *Sensors,* vol. 13, no. 7, pp. 8095-8012, 2013.

[30] J. Zheng, P. Yan, Y. Yu, Z. Ou, J. Wang, X. Chen and C. Du, "Temperature and index insensitive strain sensor based on a photonic crystal fiber inline Mach–Zehnder interferometer," *Optics Communications,* vol. 297, no. 1, pp. 7-11, 2013.

[31] F. Xu, B. Peng, D. Chen, L. Wang, X. Lei and Q. Shi, "A novel strain sensor based on a dual-core photonic crystal fiber," *Microwave and Optical Technology Letters,* vol. 56, no. 12, pp. 2778-2780, 2014.

[32] X. Bai, D. Fan, S. Wang, S. Pu and X. Zeng, "Strain sensor based on fiber ring cavity laser with photonic crystal in-line Mach-Zehnder interferometer," *IEEE Photonics Journal,* vol. 6, no. 4, pp. 1608-1612, 2014.

[33] J.M.Lopez-Higuera, Handbook of Optical Fiber Sensing Technology, New York: Wiley, 2002.

[34] P. S. J. Russell, "Photonic-crystal fibers," *Journal of Lightwave Technology,* vol. 24, no. 12, pp. 4729-4749, 2006.

[35] B. Dong and E. J. Hao, "Temperature-insensitive and intensity-modulated embedded photonic crystal fiber modal interferometer based microdisplacement sensor," *Journal of the Optical Society of America B,* vol. 28, no. 10, pp. 2332-2336, 2011.

[36] H. Gong, X. Li, Y. Jin and X. Dong, "Hollow-core photonic crystal fiber based modal interferometer for strain," *Sensors and Actuators A: Physical,* vol. 187, no. 1, pp. 95-97, 2012.

[37] F. Xu, C. Li, D. Ren, L. Lu, W. Lv, F. Feng and B. Yu, "Temperature-insensitive Mach-Zehnder interferometric strain sensor based on concatenating two-waist-enlarged fiber tapers," *Chinese Optics Letters,* vol. 10, no. 7, pp. 070603-070606, 2012.

[38] R. Jha and G. J. Villatrio, "Ultrastable in reflection photonic crystal fiber modal interferometer for accurate refractive index sensing," *Applied Physics Letters,* vol. 93, no. 191106, pp. 1-3, 2008.

[39] D. Noordegraaf, L. Scolari, J. Lægsgaard, T. T. Alkeskjold, G. Tartarini, L. Borelli, P. Bassi, J. Li and S. T. Wu, "Avoided-crossing-based liquid-crystal photonic-bandgap notch filter," O*ptics Letters,* vol. 33, no. 9, pp. 986-988, 2008.

[40] H. K. Tyagi, M. A. Schmidt, L. P. Sempere and P. S. J. Russell, "Optical properties of photonic crystal fiber with integral micron-sized ge wire," *Optics Express,* vol. 16, no. 22, pp. 17227-17236, 2008.

[41] H. W. Lee, M. A. Schmidt, H. K. Tyagi, L. P. Sempere and P. S. J. Russell, "Polarization-dependent coupling to plasmon modes on submicron gold wire in photonic crystal fiber," *Applied Physics Letters*, vol. 93, pp. 1-3, 2008.

[42] A. Nagasaki, K. Saitoh and M. Koshiba, "Polarization characteristics of photonic crystal fibers selectively filled with metal wires into cladding air holes," *Optics Express*, vol. 19, no. 4, pp. 3799-3808, 2011.

[43] B. Lee, S. Roh and J. Park, "Current status of micro- and nano-structured optical fiber sensors," O*ptical Fiber Technology,* vol. 15, no. 3, pp. 209-221, 2009.

[44] S. Jhang, X. Yu, P. Shum, Y. H. H. P. Zhang and D. Liu, "Highly sensitive pressure-induced plasmon resonance birefringence in a silver-coated photonic crystal fiber,"

in *Journal of Physics: Conference Series of International Photonics and Optoelectronics Meetings*, China, 2010.

[45] Y. Peng, J. Hou, Z. Huang and Q. Lu, "Temperature sensor based on surface plasmon resonance within selectively coated photonic crystal fiber," *Applied Optics,* vol. 38, no. 3, pp. 6361-6367, 2012.

[46] Y. Lu, M. T. Wang, C. J. Hao, Z. Q. Zhao and J. Q. Yao, "Temperature sensing using photonic crystal fiber filled with silver nanowires and liquid," *IEEE Photonics Journal,* vol. 6, no. 3, pp. 1-7, 2014.

[47] D. Chen, G. Hu and L. Chen, "Dual-core photonic crystal fiber for hydrostatic pressure sensing," *IEEE photonics Technology Letters,* vol. 23, no. 24, pp. 1851-1853, 2011.

[48] S. Zhang, X. Yu, Y. Zhang, P. Shum, Y. Zhang, L. Xia and D. Liu, "Theoretical study of dual-core photonic crystal fibers with metal wire," *IEEE photonics Journal,* vol. 4, no. 4, pp. 1178-1187, 2012.

[49] M. Skorobogatiy, K. Saitoh and M. Koshiba, "Transverse light guides in microstructured optical fibers," *Optics Letters,* vol. 31, no. 3, pp. 314-316, 2006.

[50] W. E. P. Padden, M. A. V. Eijkelenborg, A. Argyros and N. A. Issa, "Coupling in a twin-core microstructured polymer optical fiber," *Applied Physics Letters,* vol. 84, no. 10, pp. 1689-1691, 2004.

[51] H. Y. Choi, M. J. Kim and B. H. Lee, "All-fiber Mach-Zehnder type interferometers formed in photonic crystal fiber," *Optics Express,* vol. 15, no. 9, pp. 5711-5720, 2007.

[52] H. W. Lee, M. A. Schmidt, R. F. Russell, N. Y. Joly, H. K. Tyagi, P. Uebel and P. S. Russell, "Pressure-assisted meltfilling and optical characterization of Au nano-wires in microstructured fibers," *Optics Express,* vol. 19, no. 13, pp. 12180-12189, 2011.

[53] Y. Wang, C. R. Liao and D. N. Wang, "Femtosecond laser-assisted selective infiltration of microstructured optical fibers," *Optics Express,* vol. 18, no. 17, pp. 18056–18060, 2010.

[54] R. K. Verma and B. D. Gupta, "Theoretical modelling of a bi-dimensional U-shaped surface plasmon resonance basedfibre optic sensor for sensitivity enhancement," *Journal of Physics D: Applied Physics,* vol. 41, no. 9, pp. 1-6, 2008.

[55] A. K. Sharma and B. D. Rajan, "Influence of dopants on the performance of a fiber optic surface plasmon resonance sensor," *Optics Communications,* vol. 274, no. 2, pp. 320-326, 2007.

[56] Y. G. Han, Y. Chung, S. B. Lee, C. S. Kim, M. Y. Jeong and M. Kim, "Temperature and strain discrimination based on a temperature-insensitive birefringent interferometer incorporating an erbium-doped fiber," *Applied Optics,* vol. 48, no. 12, pp. 2303-2307, 2009.

[57] B. Gu, W. Yuan, A. P. Zhang and O. Bang, "All-solid birefringent hybrid photonic crystal fiber based interferometric sensor for measurement of strain and temperature," in *Asia Communications and Photonics,* Shanghai, China, 2011.

[58] G. Statkiewicz-Barabach, J. P. Carvalho, O. Frazao, J. Olszewski, P. mergo, J. L. Santos and W. Urbanczyk, "Intermodal interferometer for strain and temperature sensing fabricated in birefringent boron doped microstructured fiber," *Applied Optics,* vol. 50, no. 21, pp. 3742-3749, 2011.

[59] H. M. Kim, T. H. Kim, B. Kim and Y. Chung, "Enhanced transverse load sensitivity by using a highly birefringent photonic crystal fiber with larger air holes on one axis," *Applied Optics,* vol. 49, no. 20, pp. 3481-3485, 2010.

[60] D. Chen, "Highly birefringent four-hole fiber for pressure sensing," *Progress in Electromagnetics Research,* vol. 114, no. 1, pp. 145-158, 2011.

[61] M. A. S. Franco, V. A. Serrao, T. R. Pitarello and A. Cerqueira S. Jr., "Hybrid photonic crystal fiber sensing of high hydostatic pressure," in *21st International Conference on Optical Fiber Sensors*, Ottawa, Canada, 2011.

LIST OF PUBLICATIONS

[1] Shailly Khanna, R. S. Kaler, “Index Insensitive Micro-strain Sensor Based on a Hollow Core Photonic Crystal Fiber,” communicated to Optoelectronics and Advanced Materials - Rapid Communications (OAM-RC).

[2] Shailly Khanna, R. S. Kaler, “Response to Strain of a Metal Filled Twin-Core Photonic Crystal Fiber for Application as a Micro-strain Sensor,” communicated to Fiber and Integrated Optics Journal.

[3] Shailly Khanna, R. S. Kaler, “Sensitivity-Enhanced Micro-Strain Sensor Based on Birefringent Germanium Doped Hybrid Photonic Crystal Fiber,” communicated to Optik-International Journal for Light and Electron.

[4] Shailly Khanna, Pragya, R. S. Kaler, “Photonic Crystal Fiber Plasmonic Sensor Based on Bi-Coated Microfluidic Channels,” published in International conference on Electrical, Electronics, Computer Science and Mathematics Physical Education and Management (ICEECMPE) in New Delhi.